CHARACTERIZATION OF MICROBIAL INACTIVATION USING PLASMA ACTIVATED WATER AND PLASMA ACTIVATED BUFFER

By

ISHA JOSHI

A thesis submitted to the

Graduate School-New Brunswick

Rutgers, The State University of New Jersey

In partial fulfillment of the requirements

For the degree of

Master of Science

Graduate Program in Food Science

Written under the direction of

Professor Mukund V. Karwe and Professor Donald W. Schaffner

And approved by

_____

_____

_____

New Brunswick, New Jersey

May 2017

ABSTRACT OF THE THESIS

Characterization of Microbial Inactivation Using Plasma Activated Water and Plasma Activated Buffer

By ISHA JOSHI

Thesis Directors: Professor Mukund V. Karwe and Professor Donald W. Schaffner

Plasma activated water (PAW) has been shown to be a promising surface decontamination technique. Antimicrobial effects of PAW have been attributed to reactive oxygen and reactive nitrogen species, which act as oxidizing agents and also contribute to the acidifying effect, causing the pH of water to drop. To isolate the effect of low pH on microbial inactivation, a buffer with the same pH (3.1) as that of PAW was evaluated. Plasma Activated Buffer (PAB) was generated to study the interactive effects of low pH and plasma activated species. Previously, substrate properties (roughness) have been shown to affect the antimicrobial efficacy of plasma. The objectives of this research were: (1) To isolate the effect of pH in PAW using a buffer solution, (2) Characterize plasma, PAW, and PAB, and (3) To evaluate the effect of surface roughness on microbial inactivation using PAW and PAB.

PAW and PAB were generated by exposing sterilized distilled water and citrate-phosphate buffer (pH = 3.1), respectively, to atmospheric pressure air plasma jet. Efficacy of distilled water, PAW, buffer, and PAB for inactivation of *Enterobacter*

aerogenes was evaluated in a planktonic system, and for different surfaces with increasing roughness. Surface roughness (P_q) values for four sample surfaces (glass slide, grape tomatoes, limes, spiny gourd) were obtained using Confocal Laser Scanning Microscopy (CLSM). Optical Emission Spectroscopy (OES) was used to obtain an emission spectra for plasma. Electrical conductivity and Oxidation Reduction Potential (ORP) were measured for PAW and PAB.

In the planktonic system for treatment time of 10 min, a (1.92 ± 0.70) log CFU/ml reduction using PAW (pH = 3.1) was achieved, however, no reduction was observed using only the buffer at the same pH. This confirmed that the inactivation was due to the reactive species in PAW, and not due to the low pH. A (5.11 ± 0.63) log CFU/ml reduction was observed using PAB in the same system, suggesting interactive effects of plasma generated species and low pH in the buffer system.

In studies with glass slide, grape tomatoes, limes, and spiny gourd, it was found that as the surface roughness (P_q) value increased, the inactivation due to PAB treatment decreased. Highest reduction of (6.32 ± 0.43) log CFU/surface was achieved for glass slide (P_q = 0.28 ± 0.02 µm), followed by (5.31 ± 0.14) log CFU/surface for grape tomatoes (P_q = 5.17 ± 0.53 µm), and (3.80 ± 0.63) log CFU/surface for limes (P_q = 18.76 ± 3.00 µm). The least reduction of (2.52 ± 0.46) log CFU/surface was observed for spiny gourd, which had the highest roughness (P_q = 101.50 ± 10.95 µm). For PAW treatment, lower inactivation for each surface was observed. Moreover, no significant difference in microbial inactivation between the samples of different roughness values, was observed

when treated with PAW. The ORP and electrical conductivity values of PAW and PAB showed a positive correlation with microbial inactivation in the planktonic system.

Thus, PAW and PAB can potentially be used for fresh produce decontamination. However, further research is needed to confirm the suitability of PAW as an industrial sanitizer. In addition, the effectiveness of plasma activated organic acids also should be explored.

ACKNOWLEDGEMENTS

I take great pleasure in thanking my advisors Dr. Mukund V. Karwe and Dr. Donald W. Schaffner who have guided me with their invaluable inputs and suggestions throughout my graduate studies both on scientific and personal front. I have gained tremendously from their expertise in the domains of food engineering and food microbiology.

I would like to thank Dr. Deepti Salvi for serving on my committee and for giving valuable suggestions contributing towards my work.

I would like to acknowledge Dave Petrenka and Bill Sumal for setting up the plasma equipment, Dr. Prabhas V. Moghe and Daniel Martin of Chemical and Biochemical Engineering for the use of Confocal Laser Scanning Microscopy and Dr. Yesu Das for the use of electrical conductivity meter.

I would take this opportunity to thank all my labmates from Dr. Karwe's and Dr. Schaffner's laboratories for their thoughtful suggestions and making the laboratories a friendly and relaxing environment to work in. Last but not the least, I would like to thank my family without whom none of this would have been possible.

TABLE OF CONTENTS

LIST OF FIGURES

LIST OF TABLES

1. INTRODUCTION

1.1. Cold Atmospheric Pressure plasma

Chemist Irving Langmuir first described the term 'plasma' as plasma oscillations, when he observed specific oscillations in an ionized gas (Langmuir, 1923). When energy is provided to a solid, the relative motion between its constituent atoms and molecules increases thereby causing its transition to a liquid state. On further supply of energy, it changes to gaseous state and later into a state consisting of charged species of equal number of densities (d'Agostino et al., 2005). Plasma is thus, typically referred to as the fourth state of matter, containing partially or wholly ionized gas comprising essentially of photons, ions and free electrons as well as atoms in their fundamental or excited states possessing a net neutral charge (Misra et al., 2011; Moreau et al., 2008).

Two major types of plasma are generally identified, equilibrium plasma and non-equilibrium plasma. In a thermodynamic equilibrium plasma, electrons and ions have approximately the same temperature ($T_{ion} \approx T_{overall} \approx T_{electron}$). Electrons lose energy to ion species owing to the high collision frequency, thus providing thermalization and thermodynamic equilibrium. Such plasmas have higher ionization degree and have temperatures $\geq 10^4 K$ (Surowsky et al., 2015). They may also be referred to as thermal plasmas (Moreau et al., 2008).

Non-equilibrium state plasma, however, have ions and electrons in thermodynamic non-equilibrium. They have different temperatures, where temperature of electrons is of the order of 10^4 K, while ions and neutrals have temperatures near room temperatures. The

chemistry is driven by electrons and such plasmas exhibit low ionization degrees (Surowsky et al., 2015). They are commonly referred to as non-thermal plasmas (Moreau et al., 2008).

1.1.1. Method of Generation

Low temperature atmospheric pressure plasma can be generated in different ways, of which the most commonly reported are, corona discharge, dielectric barrier discharge, atmospheric pressure plasma jet, and microwave driven discharges. In this study, atmospheric pressure plasma jet was used to generate plasma treated liquid solutions, which were then evaluated for their antimicrobial efficacy (Ehlbeck et al., 2011).

Plasma jets are described as non-thermal capacitively coupled plasma sources that typically operate in the radio frequency range (e.g., at 13.56 MHz or 27.12 MHz) (Ehlbeck et al., 2011). They usually consist of two electrodes (e.g., a needle electrode and a grounded electrode), that may be set up in different configurations as shown in Figure 1. Typically, noble gases (e.g., argon or helium) are excited with voltages up to 100 V, while keeping the distance between the electrodes up to a few millimeters (Ehlbeck et al., 2011; Surowsky et al., 2015). The flowing gas is used to push the plasma discharge through an orifice which comes out as jet (Scholtz et al., 2015).

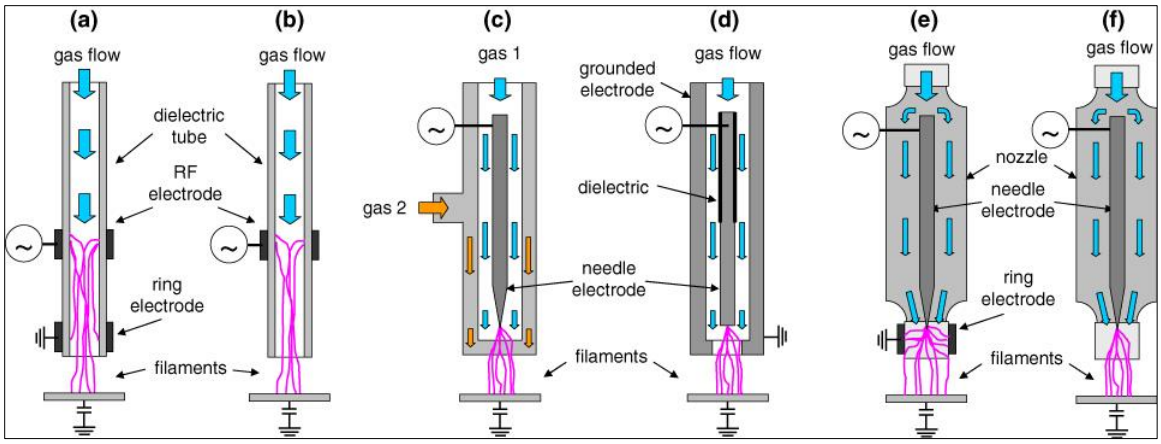

Figure 1: Different electrode configurations used for atmospheric pressure plasma jet (Source: Ehlbeck et al., 2011)

Targeted applicability allowing the plasma jet to reach narrow gaps is a major advantage for plasma jet (Surowsky et al., 2015). It has a simpler design which is easy to maintain, allowing it to be used in multiple sources such as jet, plasma pen, plasma torch, and plasma needle (Scholtz et al., 2015).

1.1.2. Application of Plasma in Various Fields

Low temperature plasma applications have increased enormously after the end of the twentieth century. It has been used in a vast variety of fields for different technological applications, such as lamps, pretreatment of polymers, sanitation of surfaces, etc. Few of the major industrial applications of plasma are as listed below (Loureiro & Amorim, 2016):

1) Automotive Industry: Low-temperature plasmas have found several applications in the automotive industry, namely,

a) Weight reduction in car windows and lenses by replacing ceramic glasses by transparent plastic material such as polycarbonate, with improved diffusion barrier properties, corrosion resistance and increased adhesion, achieved by the process of plasma polymerization.

b) Improved painting and adhesive bonding capabilities for several plastic parts for car (e.g., bumper stickers) achieved by corona treatment.

c) Diamond-like carbon (DLC) coatings for low friction coefficient for lubricant free bearings achieved by microwave plasma chemical vapor deposition (Suchentrunk et al., 1997).

2) Biomass processing: Maksimov and Nikiforov (2007) have reported feasibility for bleaching and delignification of cotton or cellulose with the use of gas plasma or liquid phase plasma.

3) Medicine and Pharmacy: Use of plasma in wound healing and tissue regeneration has been reported by many researchers. Use of plasma needle for controlled tissue coagulation was reported by Stoffels et al. (2007). von Woedtke et al. (2013), reported the use of plasma in pharmaceutical industry to achieve enhanced drug transport across cell membranes by modifying biological barrier properties, such as 'plasma poration'. Kalghatgi et al. (2015), observed higher transdermal diffusion of dextran molecules when the skin was treated with plasma. They attributed this effect to

the high electric field which may result in breakdown of the stratus corneum (outer layer of the skin), leading to formation of new channels through which the molecules could be transported.

4) Biology and Agriculture: Application of plasma technology as a decontamination technique in food systems in an upcoming field. It has been used for decontamination of juices in small volumes of 50 µL (on a cover slip) (Shi et al., 2011) and 0.8 ml (in a batch chamber) (Montenegro et al., 2002), for decontamination of shell eggs (Ragni et al., 2010), and as a new-trend for in-package decontamination (Pankaj et al., 2014).

1.1.3. Plasma Activated Water

Kamgang-Youbi et al. (2007), first studied the effect of temporal post-discharge treatment of a fluid, which he referred to as plasma-activated water, using gliding arc discharge plasma on the inactivation of *Hafnia alvei,* a type of bacteria found in human GI tract. Water was exposed to gliding arc discharge for 10 min to generate the 'plasma activated water'. They observed ~5 log CFU/ml reduction in *Hafnia alvei* when exposed to activated water for 10 min. They also observed a decrease in inactivation capacity of the activated water on storage for up to 24 h. The lethal effect of this solution was attributed to the presence of reactive species such as hydroxyl radical ($OH^{\cdot}$), nitric oxide radical ($NO^{\cdot}$), hydrogen peroxide (H_2O_2), nitrous acid (HNO_2), nitric acid (HNO_3), etc., known to be present in the plasma plume.

Table 1 illustrates some of the recent microbial inactivation studies conducted with Plasma- Activated Water (PAW).

Table 1: Illustration of microbial inactivation results using PAW.

Mode of Generation	**Substrate**	**Microorganism**	**Kill achieved**	**Reference**
Gliding arc (Feed gas: Air)	Planktonic (10 ml PAW)	*Hafnia alvei*	~ 5 log CFU/ml for 20 min exposure	Kamgang-Youbi et al., 2008
Gliding arc (Feed gas: Air)	Planktonic (10 ml PAW)	*Staphylococcus epidermidis*	~5.81 log CFU/ml for 30 min exposure	Kamgang-Youbi et al., 2009
		Leuconostoc mesenteroides	~5.88 log CFU/ml for 30 min exposure	
		Saccharomyces cerevisiae	~3.09 log CFU/ml for 30 min exposure	
Dielectric Barrier Discharge (Feed gas: Air)	Planktonic (10 ml physiological saline)	*Escherichia coli*	~6.0 log CFU/ml for 30 min exposure	Oehmigen et al., 2010
		Bacillus atrophaeus spores	~0.5 log CFU/ml for 30 min exposure	

Dielectric Barrier Discharge (Feed gas: Air)	Planktonic (1 ml PAW)	*Escherichia coli*	~5.6 log CFU/ml for 15 min exposure	Traylor et al., 2011

The microbial inactivation efficacy of PAW depends on not only the activity of chemical reactive species generated, but also on the excitation voltage, working gas and generation mode. Tian et al. (2015), observed that PAW generated by exposing plasma beneath surface of water had higher sterilization efficacy than exposing plasma above the surface of water, as shown in Figure 2. Tian et al. (2015), suggested that the higher kill achieved with PAW-B than PAW- A may be due to higher electrical conductivity and higher ORP values observed in PAW-B than PAW- A.

Figure 2: Representation of PAW generated above (left) and beneath surface (right) of water (Source: Tian et al., 2015)

United States Department of Agriculture (USDA) has also initiated a funded project with University of California, Davis, to investigate the use of plasma treated water as an alternative sanitization technology to help reduce microbial load in wash water, preserve quality of produce and thereby reduce risk of cross contamination (USDA, 2016).

Thus, further research in investigating plasma activated water as a sanitation technique is important and was a primary goal of this study.

1.1.4. Plasma-Liquid Interaction/ Plasma Chemistry

Collisions between electrons, atoms and molecules during generation of non-thermal plasma, lead to the formation of variety of reactive species, such as reactive oxygen species (e.g., atomic oxygen, hydroxyl radicals, and ozone), charged particles, electrons and VUV-UV photons. Plasma generated in gas-liquid interaction is similar to that generated in gas phase, however, presence of liquid acts as an additional electrode, giving rise to interesting plasma chemistry and reactive species (Surowsky et al., 2015). At a typical gas-liquid interface, following reactions take place:

a) Acid-base reactions
b) Oxidation reactions caused by reactive oxygen and nitrogen species
c) Reduction reactions caused by hydrogen and hydroxyl radicals
d) Photochemical reactions initiated by UV radiation from plasma.

Plasma induced ionization of water molecules leads to the formation of reactive radicals such as hydroxyl radicals (Surowsky et al., 2015; Anderson et al., 2016)

$$H_2O + e^- \rightarrow H_2O^+ + 2e^-$$

$$H_2O + e^- \rightarrow H^{\cdot} + OH^{\cdot} + e^-$$

Hydroxyl radicals may undergo combination reactions to form secondary stable products, which may also contribute to the lethal effect of PAW, such as hydrogen peroxide (Surowsky et al., 2015)

$$H^{\cdot} + OH^{\cdot} \rightarrow H_2O$$

$$OH^{\cdot} + OH^{\cdot} \rightarrow H_2O_2$$

The dissolved atomic oxygen is consumed quickly by reacting with molecular oxygen for generation of ozone (Liu et al., 2016).

$$O + O_2 \leftrightarrow O_3$$

Formation of reactive nitrogen species is known to affect the pH of the solution (Surowsky et al., 2015):

$$O_2^- + NO^{\cdot} \rightarrow (O = N - OO^{-\cdot})$$

$$NO_2^- + H_2O_2 \rightarrow (O = N - OO^{-\cdot}) + H_2O$$

$$OH^{\cdot} + NO_2 \rightarrow (O = N - OO^{-\cdot}) + H^+$$

Peroxynitrite ($O = N - OO^{-\cdot}$) is a strong peroxidizing agent and is formed most favorably from recombination reaction of nitrite radical and hydrogen peroxide, since it is found in gas-liquid environment (Surowsky et al., 2015).

Thus, multiple short-lived (OH, O_2^-, HO_2, NO_3) and long-lived ($H^+, nitrate, nitrite, H_2O_2, and\ O_3$) reactive oxygen and reactive nitrogen species, are generated by heterogeneous mass transfer in PAW and PAB, giving rise to its complex liquid chemistry and contributing to its antimicrobial efficacy.

1.1.5. Microbial Inactivation Mechanism

The antimicrobial efficacy of Plasma activated water has been attributed to the presence of reactive oxygen species (ROS), reactive nitrogen species (RNS) (Tian et al., 2015) and hydrogen peroxide (Burlica et al., 2010). The mechanisms for each have been explained in detail as follows:

a) Oxidative stress caused by Reactive Oxygen species (ROS)

Charge exchange reactions involving ions and neutrals results in the formation of several reactive oxygen species such as atomic oxygen, hydroxyl radical, and ozone. Reactions of these activated oxygen species with hydrocarbon bonds is known to weaken the cell wall of bacteria (Chau et al., 1996). Oxidative stress resulting in reduced membrane potential, leading to breach of cell membrane causing cytosolic leakage has also been suggested which may lead cell death (Joshi et al., 2011).

Interaction of reactive oxygen species with lipids in cell membrane result in lipid peroxidation process, as explained below (Gaunt et al., 2006).

Initiation:

Carbon-centered lipid radical ($L^{\cdot}$) and water molecule are produced when hydrogen is abstracted from the side chain of an unsaturated fatty acid (L) by a radical

$$L + OH^{\cdot} \rightarrow L^{\cdot} + H_2O$$

Propagation:

Lipid peroxyl radical ($LOO^{\cdot}$) is formed on when lipid radical reacts with oxygen molecule,

$$L^{\cdot} + O_2 \rightarrow L - OO^{\cdot}$$

Lipid peroxyl radical abstracts hydrogen from unsaturated fatty acid to form another peroxyl radical, thereby continuing the chain reaction,

$$L - OO^{\cdot} + L \rightarrow L^{\cdot} + LOOH$$

Lipid hydroperoxides will give rise to lipid alkoxy radicals via Fenton reaction, and short chain aldehydes via fragmentation

$$LOOH \xrightarrow{Fe\ or\ Cu} L - O^{\cdot}$$

Termination:

Radicals react with each other to form non-radical products. Anti-oxidants such as α-tocopherol may terminate reaction by scavenging peroxyl radicals.

Lipid peroxidation generates shorter products than the initial unsaturated fatty acid in the cell membrane. Unsaturated fatty acids increase membrane fluidity (due to presence of double bonds), which affects the structural integrity of the membrane, leading to osmotic imbalance and ultimately cell lysis. Moreover, aldehydes formed during these reactions are extremely reactive and may damage protein (Gaunt et al., 2006).

b) Reactive Nitrogen Species

Reactive Nitrogen Species (RNS) is a collective term that is used to refer to different nitrogen based species such as nitric oxide radical ($NO^{\cdot}$), peroxynitrite ($ONOO^{-}$), nitrogen dioxide radical ($NO_2^{\cdot}$), and other oxides of nitrogen (Dhawan, 2014).

Peroxynitrite radical exhibits bactericidal activity because of its ability to diffuse through cell wall and cause cell damage due to its ability to initiate lipid peroxidation. Its conjugate acid, peroxynitrous acid, also is a strong oxidant and shows ability to react with biological molecules (Van Gils et al., 2013).

Oehmigen et al. (2010), suggested that nitric acid formation in plasma water may contribute towards acidification of water. Moreover, nitrous acid is also known to decompose to nitric acid on reaction with hydrogen peroxide, probably contributing to the acidification. Both nitrous and nitric acid are known to have bactericidal properties

(Dhawan, 2014). Schnabel et al. (2014), suggested that etching mechanism may also play a role in microbial inactivation due to the corrosive and toxic action of nitrogen dioxide radical ($NO_2^{\cdot}$).

c) Hydrogen Peroxide

Hydrogen peroxide is a secondary reactive compound, and a strong oxidizing agent. It has been known to possess antimicrobial effects, mainly due to its oxidizing power and ability to damage DNA following the Fenton reaction (Burlica et al., 2010). Haber and Weiss (1934) first suggested the reaction between hydrogen peroxide and superoxide radical (O_2^-) (a conjugate of perhydroxyl radical), which formed to be the basis of cytotoxicity of hydrogen peroxide.

$$O_2^{\cdot -} + H_2O_2 \rightarrow O_2 + OH^- + OH^{\cdot}$$

Furthermore, the production of short-lived hydroxyl radicals proceeding through the Fenton reaction, in presence of ferrous iron, supplements the antimicrobial effect since hydroxyl radical itself is a very strong oxidizing agent (Linley et al., 2012).

$$Fe^{2+} + H_2O_2 \rightarrow Fe^{3+} + OH^- + OH^{\cdot}$$

$[4Fe\text{-}4S]^{2+}$ cluster containing enzymes are the main targets for ROS. O_2^- and H_2O_2 catalyze the release of ferric (Fe^{3+}) ions from iron-sulphur centers, since they can freely penetrate the enzymes. Moreover, free unincorporated or DNA associated ferrous (Fe^{2+}) ions also undergo oxidization due to H_2O_2 via Fenton reaction. Resulting hydroxyl radicals cause DNA oxidative damage by attacking either at base or sugar residues (Mertens and Samuel, 2012).

Thus, plasma activated water exhibits strong antimicrobial efficacy owing to the different mechanisms associated with the reactive species produced in it.

1.2. Post-Harvest Processing of Fresh Produce

Different post-harvest technologies are applied to harvested fruits and vegetables to ensure food safety, minimize losses between harvest and consumption, and to maintain the quality of the fresh produce. Typically harvested crops are processed at a packing house before they reach retail market. A typical process carried out in a packing house consists of the following steps (as explained in Figure 3) (Kitinoja & Kader, 2002),

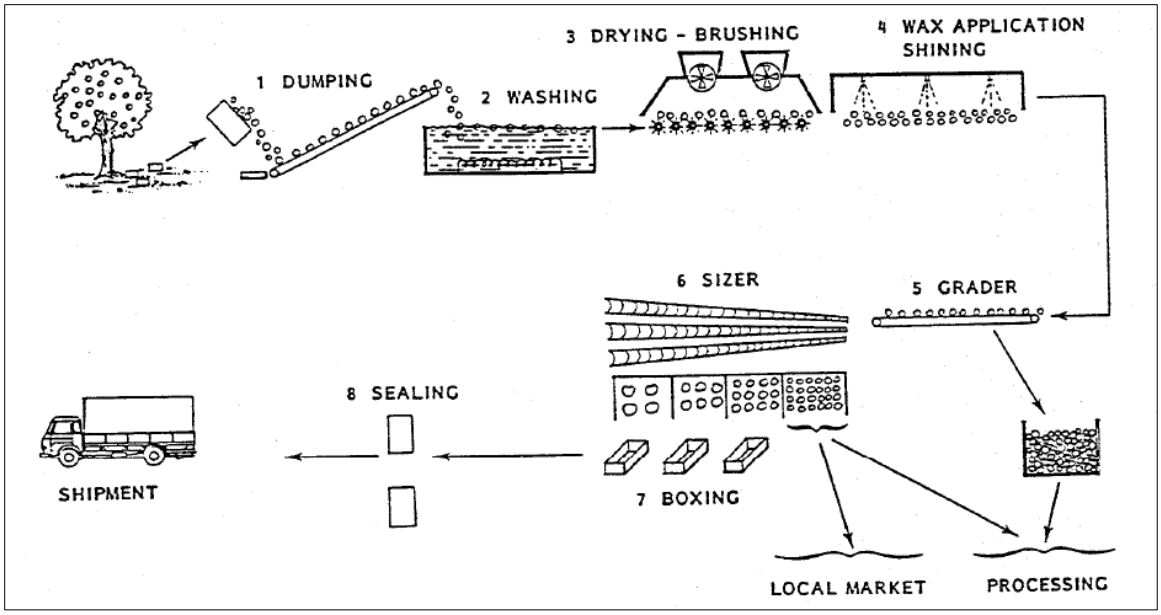

Figure 3: Typical packing house operation (Source: FAO, 1986)

a) Dumping

b) Pre-sorting: to eliminate injured, decayed or defective produce

c) Cleaning: Washing (tomatoes, leafy greens, bananas) or air-brushing (onions, garlic), depending on the type of produce. Chlorine (100 ppm - 150 ppm) may be used for washing.

d) Waxing: to help reduce water loss

e) Sizing: based on U.S. grades and standards

f) Shipment to retail market

Washing step during post-harvest handling is an important step that dictates the safety of the produce.

1.2.1. Current Practices of Fresh Produce Sanitation used in the Industry

Post harvesting, most fresh produce is subjected to a washing process to facilitate removal of organic load, lower produce temperature, and reduce surface microbial load, to achieve improved quality and shelf life. Washing may be done using batch tanks or water sprays, with a common practice of recycling the wash water for conservation. However, this practice may result in cross-contamination, adversely affecting produce batches (Herdt and Feng, 2009). Several antimicrobial agents have been approved by U.S. Food and Drug Administration (FDA) for use in fruit washing, which are listed as follows:

1) Chlorine: Free available chlorine refers to chlorine gas (Cl_2), hypochlorous acid ($HClO$) or hypochlorite ions (ClO^-). The main ingredient formed is hypochlorous acid. Lethality of hypochlorous acid is due to its interactions with cell membrane proteins,

which results in the formation of nitrogen-chlorine based derivatives, which are hypothesized to interfere with cell metabolism. For a sanitation treatment, typical chlorine concentration used is 200 mg/ L at pH < 8.0 for 1 min - 2 min contact time washing cycle. Although efficiency of chlorine is higher at low pH (4-5), it is typically used at pH 6.5-7.0, due to the corrosive action of low pH for the equipment (Herdt and Feng, 2009).

2) Electrolyzed water: Electrolysis of water containing a low concentration of sodium chloride (0.1 %) in a chamber containing anode and cathode, separated by bipolar membrane, gives electrolyzed water. Two streams generated are,

a) Acidified Electrolyzed water (AEW): It is generated at anode and typically has pH < 2.6, oxidation-reduction potential (ORP) of > 1100 mV and has hypochlorous acid present.

b) Basic Electrolyzed water (BEW): It is generated at cathode and typically has a pH of > 11.4 and an ORP value of < -795 mV.

AEW has been reported to be used for sanitizing eggs and in the brewing industry in the United States of America (Herdt and Feng, 2009).

Electrolytically generated hypochlorous acid (also known as Electrolyzed water) has been approved as an antimicrobial agent used to re-hydrate fresh and fresh-cut fruits and vegetables, given that the free chlorine will not exceed 60 ppm (FDA, 2015b). It has also been approved by USDA to be used as a spray for processing contaminated poultry carcasses given that the free chlorine content does not exceed 50 ppm (USDA, 2017).

3) Acidified Sodium Chlorite: It is formed by combination of sodium chlorite with a weak acid like citric acid in aqueous solution. Controlled conditions allow higher production of hypochlorous acid than chlorine dioxide. It is generally combined with any GRAS acid to produce a pH between (2.3-2.9) and a chlorite concentration of 500 ppm to 1200 ppm. Fruit washing with sodium chlorite must be followed by potable water rinse or blanching (Herdt and Feng, 2009).

4) Ozone: Ozone acts as a strong oxidizer and affects the cell permeability resulting in cell lysis and death. Although ozone was declared as Generally Recognized As Safe (GRAS) in 1997 for food contact applications, it has the drawback of off-gassing and high sensitivity to organic load (Herdt and Feng, 2009).

5) Organic acids: Typically, several organic acids, namely, acetic acid and citric acid, are GRAS and are used to adjust pH of water in chlorine washing application. Although organic acids are very stable in presence of organic load, they are relatively expensive and can affect the organoleptic properties of fresh produce due to low pH (Herdt and Feng, 2009).

1.2.2. Factors Affecting Efficacy of Sanitizers

Efficacy of antimicrobial reagents used for produce sanitation may be affected by their mode of action (chemical, mechanical, physical). Several factors related to the antimicrobial agent (pH, concentration), produce (surface characteristics, soil load on surface) or microorganism (type, level, attachment), may affect the efficacy, and thus,

must be considered when optimizing the washing process. Herdt and Feng (2009), have described certain factors that affect the antimicrobial activity for produce washing, as listed:

1) Washing conditions:

    a) Antimicrobial concentration:

Typically, if the pH, organic load, and temperature are kept constant, high concentration of antimicrobial, results in high antimicrobial activity. However, high loads may affect produce tissue and may be an environmental issue (Herdt and Feng, 2009). The level of antimicrobial agents allowed for their use on fruits and vegetables is regulated by the U.S. Food and Drug Administration (FDA) and the Environmental Protection Agency (EPA) (e.g., 3 ppm of chlorine dioxide is allowed for contact with food produce) (FDA, 2014).

    b) Time:

A two-stage strategy used in industrial produce wash, employs two washes of 30 seconds to 1 min or 2 min each, first to remove soil and debris, followed by a second wash to remove microbial load (Herdt and Feng, 2009).

    c) Temperature:

Industrially, the water used for washing is maintained at 4 ˚C, to ensure maximum chlorine solubility. This also helps establish a temperature difference between wash water and produce (Herdt and Feng, 2009). Beuchat (1998) mentioned that a

temperature difference of 10 ˚C or higher between wash water and produce helps reduce product wash water uptake, serving to be a critical point in produce contamination.

d) pH:

For the antimicrobial agent to be effective, the pH of the solution must be below the dissociation constant of the acid used. Low pH favors bactericidal activity of wash water due to increased formation of hypochlorous acid in chlorine wash (Herdt and Feng, 2009).

2) Water Quality:

Since most antimicrobial agents are strong oxidizers, they may react with the organic matter leading to depleted effectiveness of the antimicrobial agent. Thus, it is critical to understand the interaction of antimicrobial agent and organic load, to evaluate its efficacy.

3) Microbial Type, Level, and Attachment:

Spore forming bacteria are more resistant to antimicrobial treatments than vegetative cells. Moreover, removal and inactivation of microbial biofilms on produce surface is considered to be a major challenge for the food industry (Herdt and Feng, 2009). No significant literature has been published to evaluate the efficacy of Plasma activated water against gram positive bacteria and gram negative bacteria.

4) Produce surface properties:

Interaction between produce and microorganism is greatly affected by the chemical, physical, and topographical surface properties of fresh produce. Presence of cuticular waxes, broken trichomes, scars on plants, all influence the interaction of plant and microorganism (Herdt and Feng, 2009). Wang et al. (2009), showed a positive correlation between increased surface roughness and residual bacterial population, suggesting that grooves or cavities within the fruit surface provide protection to bacterial cells against the washing treatments. As illustrated in Figure 4, Bhide (2016), showed the attachment of *E. aerogenes* in between the grooves of sandpaper of increasing roughness with from grit 600 (finer) to grit 400 (coarser), using SEM images.

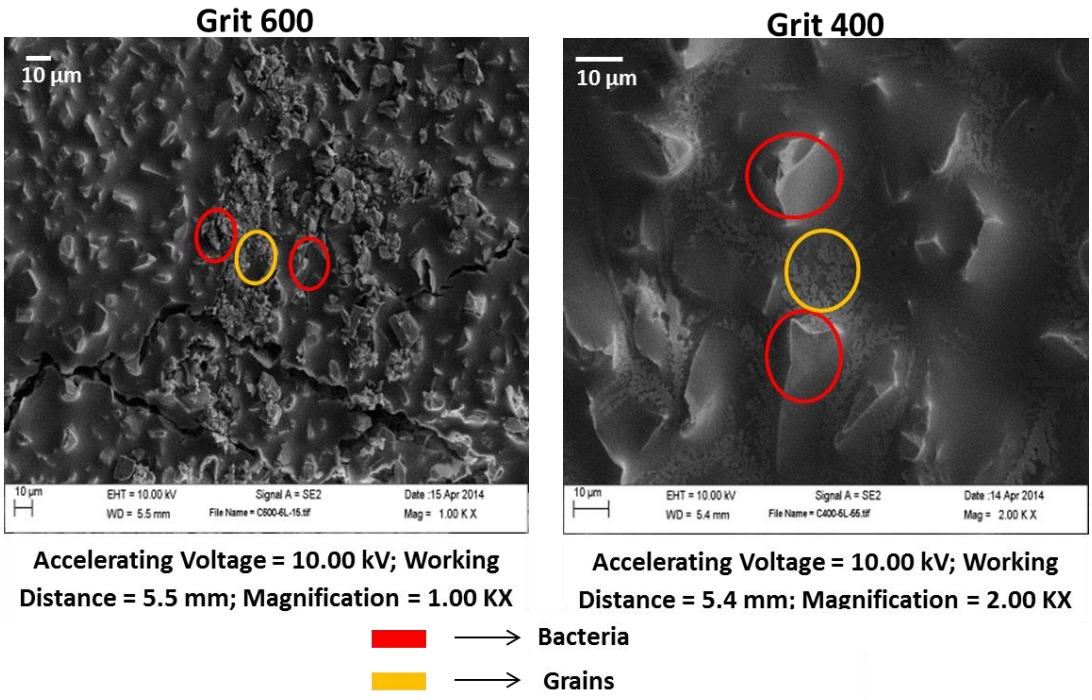

Figure 4: Attachment of *Enterobacter aerogenes* in between grooves of sandpaper of increasing roughness (Grit 600 and Grit 400) (Bhide, 2016)

The higher roughness of grit 400 sandpaper (P_q = 11.71 μm ± 1.18^b μm) than grit 600 (P_q = 6.71 μm ± 0.58^a μm) provides grooves or cavities for bacterial cells to hide and thereby report lower inactivation of *E. aerogenes* ((1.86 ± 0.12) log CFU for grit 400 sandpaper, (2.08 ± 0.2) log CFU for grit 600 sandpaper) using cold atmospheric pressure plasma (Bhide, 2016). Bhide (2016) also studied inactivation of *E. aerogenes* using cold atmospheric pressure plasma, on fruit surfaces with increasing roughness values, apples (P_q = 6.12 μm ± 2.88^a μm), oranges (P_q = 13.07 μm ± 5.26^b μm) and cantaloupes (P_q = 16.98 μm ± 6.74^c μm). Lower microbial inactivation was achieved as the roughness was increased ((1.86 ± 1.27)^a log CFU/fruit, (0.77 ± 0.86)^b log CFU/fruit, (0.61 ± 0.78)^c log CFU/fruit, for apples, oranges, and cantaloupes, respectively, which were significantly different from each other ($p<0.05$) as denoted by different superscript letters).

Thus, surface roughness play a major role in determining the efficacy of the antimicrobial treatment.

1.3. Surface Roughness

MacDevin (2007), defines surface roughness as “small scale morphology or ‘shape’ of a surface”, wherein a three-dimensional surface profile consists of peaks, valleys, ridges and grooves. Dove et al. (1996), refer to the same ‘peaks, valleys and side-slopes’ as the topography of the surface that constitute a certain ‘texture’. Figure 5 describes the terminology used to describe topography of a surface.

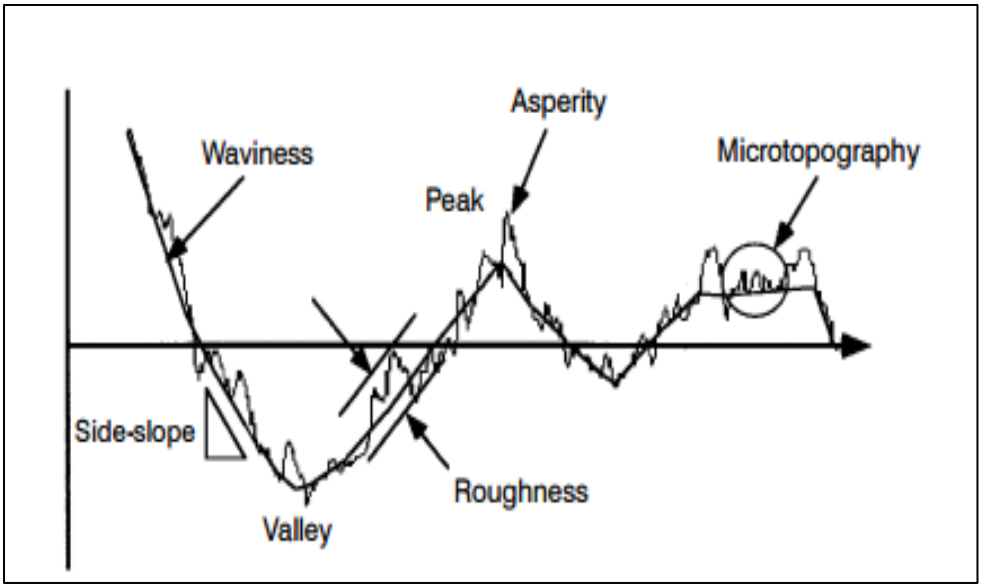

Figure 5: Terminology used to describe surface topography (Dove et al., 1996)

According to Dove et al. (1996), superimposed images of different wavelengths are used to make up the topography of most real surfaces. The term “waviness” is used to define long wavelength, higher amplitudes undulations on which a series of short wavelength, lower amplitude irregularities are superimposed. The surface roughness characteristics are constituted by these short wavelength irregularities. The application and the scale of interest dictate the length at which waviness becomes roughness. A localized region of a superimposed image consisting of a peak of an asperity, side-slope or valley of a surface profile is referred to as ‘Micro-topography’ (Dove et al., 1996).

Different definitions and parameters used to determine surface characteristics are specified by ISO 4287:1997 (ISO, 1997) (Figure 6) and are described as:

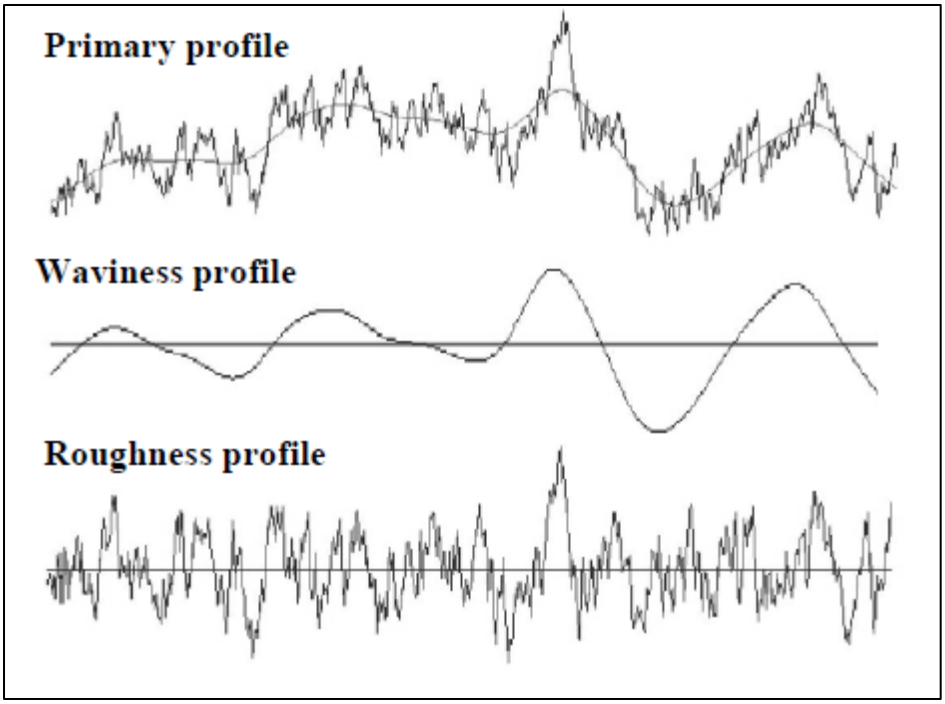

Figure 6: Roughness and waviness profile representation (ISO, 1997; Beckert and Reitz, 2012)

Primary profile: It is representative of the real surface and is the basis for evaluation of the primary profile parameters (P profile).

Roughness profile: It is profile derived from the primary profile by suppressing the long wave component (waviness); this profile is intentionally modified. It is used for evaluation of roughness parameters (R profile).

Waviness profile: It is profile derived from the primary profile by suppressing the shortwave component (roughness); this profile is intentionally modified. It is used for evaluation of waviness parameters (W profile).

All the profiles have the same transmission characteristics, but different cut-off wavelengths (ISO, 1997).

Approximately, 23 different international standards of roughness have been defined, however, most of these standards are application specific. The standards widely used for quantifying roughness are as listed below (Dove et al., 1996):

1) Average roughness (P_a /R_a /W_a): it represents the average of the asperity heights along a base centerline.

$$P_a/R_a/W_a = \left(\frac{1}{L}\right)\int_0^L |z(x)|dx \qquad \text{(Equation 1)}$$

Where, z= profile height; L= sampling length (Dove et al., 1996)

P_a /R_a /W_a are the most commonly used parameters are repeatable (B. C. MacDonald & Co., 2010).

2) Root mean square roughness (P_q /R_q /W_q): It represents the standard deviation of the asperity heights above and below the base line. P_a /R_a /W_a and P_q /R_q /W_q are sufficient to completely characterize the surface characteristics if the distribution of asperity heights is normal (Dove et al., 1996).

$$P_q/R_q/W_q = \sqrt{\left(\frac{1}{L}\right) * \int_0^L z^2(x)dx} \qquad \text{(Equation 2)}$$

P_q /R_q /W_q are more sensitive to peaks and valleys than P_a /R_a /W_a, since the amplitudes are squared and are hence used in scientific measurements (B. C. MacDonald & Co., 2010).

1.4. Fresh produce

U.S. FDA defines fresh fruits and vegetables as “Fresh produce that is likely to be sold to consumers in an unprocessed (i.e., raw) form. Fresh produce may be intact, such as whole strawberries, carrots, radishes, or tomatoes, or cut from roots or stems during harvesting, such as celery, broccoli, lettuce, or cauliflower” (FDA, 2008). In a paper published by Centers for Disease Control and Prevention (CDC) in 2013, it was stated that more than 9 million foodborne illnesses caused by major pathogens are reported in the United States every year (CDC, 2013; Painter et al., 2013). Over a span of 11 years from 1998-2008, a total of 13,352 foodborne disease outbreaks, causing 271,974 illnesses, were reported in the United States. Produce (comprising of fruits and vegetables) accounted for 46% of these illness, contributing to 38% of the annual hospitalizations and 22% of annual deaths reported domestically. Despite advances in food safety, these reports suggest that efforts are particularly needed in preventing contamination for food commodities, especially produce and poultry (Painter et al., 2013). Table 2 lists the major produce (foodborne) outbreaks reported by CDC in the last five years (CDC, 2017).

Table 2: List of foodborne outbreaks reported in last five years (CDC, 2017).

Year	Commodity	Pathogen	# of States affected	# of People affected
2016	Alfalfa sprouts	Shiga toxin-producing *Escherichia coli* O157 (STEC O157)	2	11
	Alfalfa sprouts	*Salmonella* Muenchen *Salmonella* Kentucky	12	26
	Alfalfa sprouts	*Salmonella* Reading *Salmonella* Abony	9	36
2015	Cucumbers	*Salmonella* Poona	40	907
2014	Bean Sprouts	*Salmonella* Enteritidis	12	115
	Cucumbers	*Salmonella* Newport	29	275
	Cilantro	*Cyclospora cayetanensis*	19	304
2013	Fresh produce (salad mix)	*Cyclospora cayetanensis*	25	631
	Cucumbers	*Salmonella* Saintpaul	18	84
2012	Cantaloupe	*Salmonella* Typhimurium *Salmonella* Newport	24	261
	Clover sprouts	Shiga Toxin-producing *Escherichia coli* O26	11	29

Fresh cut produce, defined as, “fresh fruits and vegetables for human consumption that have been minimally processed and altered in form by peeling, slicing, chopping, shredding, coring, or trimming, with or without washing, prior to being packaged for use by the consumer or a retail establishment,” has created a niche market for itself in the fresh produce industry. It has reached almost $12 billion in annual sales and is touted to be the fastest growing sector of fresh produce industry (FDA, 2008). Minimal processing of fresh produce, followed by absence of cooking before consumption of products such as fresh cut produce, increases the need for the food industry to come up with alternative technologies that not only help achieve food safety but also maintain ‘freshness’ of the produce. Studies based on evaluating the efficacy of nonthermal techniques such as cold atmospheric plasma and plasma activated water are a step further in that direction.

1.5. Equipment and Assays

1.5.1. Confocal Laser Scanning Microscopy (CLSM)

A confocal laser scanning microscope is used to obtain three-dimensional (3D) information of an object by scanning the object point by point using a point source laser and measuring the data using a detector only in the focal plane of the light source (Houpt and Draaijer, 1989). Using CLSM, a stack of optical sections can be reproduced by obtaining a single optical section at one focal length and then moving the focal plane along the depth of the 3D specimen at defined step (in size of µm). Either the epi-

fluorescence or the epi-reflection mode can be used for imaging using CLSM (Dürrenberger et al., 2001).

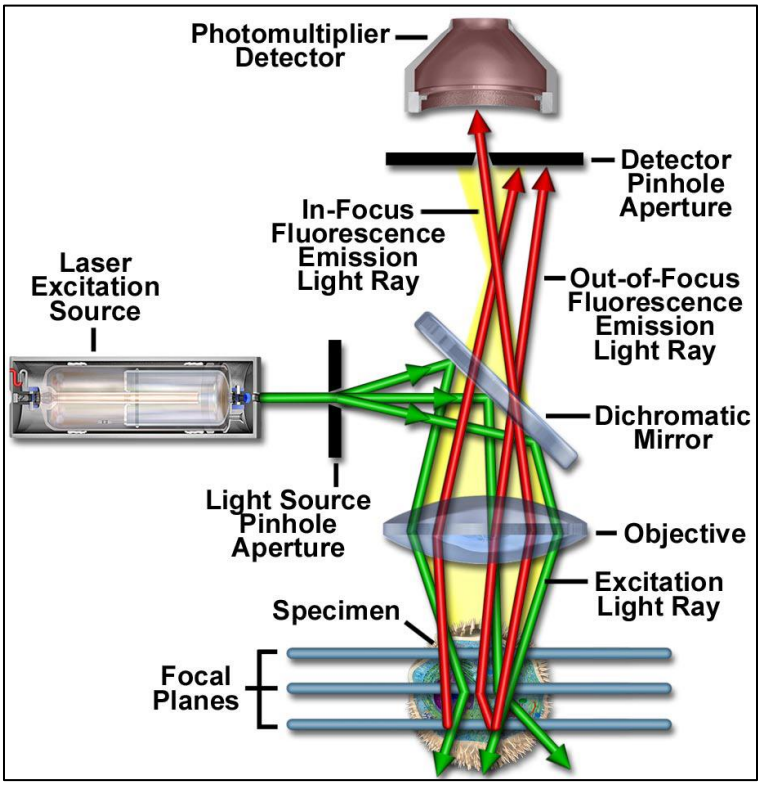

Figure 7: Schematic diagram of working principle of CLSM (Claxton et al., 2006)

Figure 7 represents a schematic of a CLSM working in the epi-fluorescence mode. A laser system is used as the excitation source (Claxton et al., 2006) to emit a collimated polarized laser beam which is deflected stepwise in the x-y direction by a scanning unit. A dichromatic mirror is used to deflect the beam to allow it to pass through the objective lens and further focus on to the specimen. The emitted longer-wavelength fluorescent light (or reflected light in reflection mode) is collected by the objective lens, passed through the dichroic mirror. It is then focused into a small pinhole near the detector to eliminate out-of-focus light. An analogue output from the detector is

digitized to a pixel-matrix form to obtain an image of the stacks of optical sections. This helps CLSM achieve excellent resolution (in this study, the resolution achieved for the set parameters was 202 nm, in the direction perpendicular to the focal plane) for a plane of section and within different section planes (Dürrenberger et al., 2001).

CLSM has been used by several researchers to obtain microstructure imaging of butter (Blonk and Aalst, 1993), freshly cut yam, wheat dough, and cooked spaghetti (Dürrenberger et al., 2001). It has also been used for obtaining surface roughness quantification of alfalfa, broccoli and radish seed surfaces (Fransisca and Feng, 2012), fresh cut cheese, ham and salami (Sheen et al., 2008) and apples, avocados, oranges and cantaloupes (Wang et al., 2009).

In our study, CLSM was used to measure surface roughness for glass surface, grape tomatoes, limes, and spiny gourd.

1.5.2. Optical Emission Spectroscopy

Optical Emission Spectroscopy (OES) (as shown in Figure 8) is the most commonly used probe for plasma diagnosis. It helps provide information on relative concentration of plasma species such as Reactive Oxygen Species (ROS) and Reactive Nitrogen Species (RNS). It also shows possibilities to be used for investigating the electron densities during plasma generation (Surowsky et al., 2015).

Figure 8: Black-Comet UV-VIS Spectrometer (left) with probe (right)

The quartz fiber optic cable has a probe that helps measure dispersed emission spectra of excited atoms to determine analyte concentration. Light is emitted in terms of spectral lines when excited analyte atoms decay to their lower energy levels. These spectral lines generated at different wavelengths are detected simultaneously by the spectrometer to generate a spectrum for the element. If the composition of substance is known, it can help identify the element (Bai et al., 2011; Chemicool, 2017).

Thus, OES serves to be a non-intrusive, inexpensive instrument that allows measurement of light emitted from atoms, molecules, and ions as a function of wavelength (100 nm - 900 nm), time, and location. In our study, OES was used to relatively quantify and identify peaks of important species generated during plasma with the help of National Institute of Standards and Technology (NIST) atomic spectra database (Surowsky et al., 2015).

1.5.3. Electrical Conductivity

Electrical conductivity is a measure of how well the solution can conduct electricity. Aqueous solutions are the basis for most conductivity measurements and the presence of charged particles or ions helps the solutions carry electric current. The presence of, ions from electrolytes in water, are responsible for the solution electrical conductivity. Electrical conductivity measures total active species present in the solution and is not specific towards certain electrolytes or ions.

Electrical conductivity is commonly used to monitor water quality, since the buildup of ionic solids in water systems and boilers may result in higher conductivity suggesting potential harmful accumulation of solids. The units of electrical conductivity are Siemens per cm (S/cm).

Contacting conductivity (S/cm) used for measuring solution conductivity, involves use of sensors consisting of two metal electrodes. An alternating voltage applied between the two electrodes sets up an electric field causing the ions to move back and forth in the solution generating an ionic current (Emerson Process Management, 2010). The cations move towards the negative electrode and the anions move towards the positive electrode, while the solution acts the conductor. Higher conductivity measurements indicate presence higher concentration of ions in the solution (Radiometer analytical SAS, 2004).

1.5.4. Oxidation Reduction Potential

Oxidation Reduction Potential is a measurement and control of oxidation-reduction reactions, wherein substances lose or gain electrons (Oliver et al., 1994). It measures the capacity of a substance to oxidize or reduce another substance. Oxidation is the loss of electron by an atom, ion or a molecule, while, reduction is the gain of electron by an atom, ion or a molecule. For example, in a redox couple Fe^{2+}/Fe,

$$Fe = Fe^{2+} + 2e^{-}$$

Iron (Fe) gets oxidized (by loss of electron) to form Ferrous ion (Fe^{2+}), which in turn shows the reduced form (gain of electron) (Emerson Process Management, 2008). An oxidation-reduction reaction is thus characterized by electron exchange (Oliver et al., 1994). Standard potential (E°) of a redox couple, helps determine how easily a substance is reduced or oxidized. Redox couple of hydrogen ion/hydrogen (H^{+}/H_2) is assigned a standard potential of zero millivolts (Tian et al., 2015; Xu et al., 2016; Jin et al., 2016).

An ORP sensor consists of a ORP electrode (usually an inert metal electrode with low resistance that can easily give or receive electrons) and a reference electrode (silver-silver chloride electrode) similar to a pH sensor. The ORP electrode continues to receive or donate electrons till it results in a build of charge, developing a potential similar to the ORP of the solution. Typically, the sensitivity of a ORP sensor is ±5 mV (Tian et al., 2015; Xu et al., 2016; Jin et al., 2016).

In this study, ORP is used to indicate the level of reactive oxygen species generated in plasma activated water and plasma activated buffer, which are known to have antimicrobial effect (Tian et al., 2015; Xu et al., 2016; Jin et al., 2016).

1.5.5. Hydrogen peroxide assay

Hydrogen peroxide is an important secondary reaction product formed during plasma-water (liquid) interaction, as explained in section 1.1.5. Quantification of hydrogen peroxide generated in plasma activated water and plasma activated buffer was done using a spectrophotometric method, first described by Eisenberg (1943).

Hydrogen peroxide is allowed to react with titanium sulfonate reagent to form a yellow-colored compound, pertitanic acid (H_2TiO_4) (Eisenberg, 1943). A modified protocol of Satterfield and Bonnel (1955), was followed to avoid interferences by other compounds in water. Working under strong acidic conditions (using sulfuric acid) allows the method to be pH independent. In presence of nitrite, to avoid decomposition of hydrogen peroxide by nitrites under acidic conditions, sodium azide solution is added before mixing with titanium sulfate reagent. Under acidic conditions, nitrites are reduced to molecular nitrogen due to reaction with sodium azide, thereby preventing any interferences from nitrites.

$$Ti^{++++} + H_2O_2 + 2H_2O \rightarrow H_2TiO_4 + 4H^+$$

The reaction is instantaneous and produces yellow color. The color developed can stay stable for up to 6 h. The yellow color intensity follows a linear relationship with hydrogen peroxide concentration, as explained by Beer- Lambert's law (Machala, 2013).

1.6. Rationale, Objectives, Hypothesis

Past research has shown that plasma activated water has the potential to be used as a sanitation technique for mushrooms and strawberries (Ma et al., 2015; Xu et al., 2016). The inactivation efficacy of plasma has been attributed to the presence of reactive oxygen species, reactive nitrogen species, and secondary reaction products such as hydrogen peroxide. Acidification of water on plasma treatment may be attributed to the presence of reactive nitrogen species such as nitric acid, however, more research needs to be conducted to isolate the effect of this acidification on the microbial inactivation efficacy of plasma.

Different plasma systems may be used to generate plasma treated water. Thus, it is necessary to define and characterize the PAW generated to allow replication on the results with different generation systems.

Previous studies with cold atmospheric plasma jet (Bhide, 2016) have highlighted the effect of surface roughness of fruits on the microbial inactivation efficacy of plasma. However, Bhide (2016), studied plasma and not PAW. Surface tension affecting the wettability of these surfaces may play a role in determining the effect of roughness in microbial inactivation efficacy of PAW.

The objectives of this research were: (1) To isolate the effect of pH in Plasma Activated Water using buffer solution, (2) To characterize plasma, plasma activated water, and plasma activated buffer, and (3) To evaluate the effect of surface roughness on microbial inactivation using Plasma Activated Water and Plasma Activated Buffer.

2. MATERIALS AND METHODS

2.1. Materials

2.1.1. Bacterial Culture (*Enterobacter aerogenes*)

Nalidixic acid resistant *Enterobacter aerogenes* B 199A (VivolacCultures, Indianapolis, Indiana, USA) was used in this research. This non-pathogenic strain of *Enterobacter aerogenes* has been shown to have similar attachment characteristics as *Salmonella* spp. (Zhao et al., 1998) and has been used by researchers previously in cross-contamination studies as a non-pathogenic surrogate for *Salmonella* spp. (Chen et al., 2001). *E. aerogenes* is a gram-negative bacterium like *Salmonella* (Liu and Schaffner, 2007) and nalidixic acid resistance of this strain allows it to be easily enumerated in presence of background microflora (Chen et al., 2001).

2.1.2. Media for Culturing *E. aerogenes*

2.1.2.1. Glycerol Stock for *E. aerogenes* storage

Eighty percent glycerol (Glycerol, Certified ACS solution, Fisher Scientific, USA) solution was used for storage of *E. aerogenes* at sub-zero temperatures. The solution was autoclaved at 121 °C for 15 min and allowed to cool. Tryptic Soy Broth (Soybean-Casein Digest Medium) was used to grow *E. aerogenes* by incubating for 24 h at 37 °C. A sterile micro centrifuge tube was used to mix 0.5 ml of this culture and 0.5 ml of prepared glycerol stock and stored at -80 °C for further use.

2.1.2.2. Nalidixic Acid Solution

Ten milliliters stock solution of Nalidixic acid was prepared in a 10 ml sterile conical centrifuge tube. One half of a gram of Nalidixic acid (Fisher BioReagents, USA) was dissolved in a mixture of 2 ml 10 N Sodium Hydroxide solution (Fisher Science Education, USA) and 8 ml of distilled water in a centrifuge tube. The solution was passed through a 0.22 µm sterile filter unit with MF-Millipore™ MCE Membrane (Millex® -GS) (Merck Millipore Ltd., Ireland). Final concentration of 50 µg/ml nalidixic acid was used in this research study.

2.1.2.3. Tryptic Soy Agar

Difco™ Tryptic Soy Agar (Becton, Dickinson & Company, USA) was prepared by adding 40 g of Difco™ Tryptic Soy Agar powder to 1 L of distilled water. Sterile solution was obtained by autoclaving at 121 °C for 15 min. Nalidixic acid was added after allowing the solution to cool down to 45 °C - 50 °C, to give a concentration of 50 µg/ml. Approximately 25 ml of solution was poured into sterile petri plates (Fisherbrand® Petri plates, Stackable lids, Fisher Scientific, USA), which were then used for microbial enumeration.

2.1.2.4. Tryptic Soy Broth

Bacto™ Tryptic Soy Broth (Soybean- Casein Digest Medium, Becton, Dickinson & Company, USA) was prepared by adding 30 g of Bacto™ Tryptic Soy Broth powder to 1 L

of distilled water and autoclaving at 121 °C for 15 min. Nalidixic acid was added after allowing the solution to cool down to 45 °C - 50 °C, to give a concentration of 50 µg/ml.

2.1.2.5. One Tenth Percent Peptone Water

0.1% Difco ™ Peptone water was prepared by dissolving 1.5 g of Difco ™ Peptone powder (Becton, Dickinson & Company, USA) in 1 L of distilled water. Nine ml solution was poured into glass test tubes to be further used for serial dilution. Sterile solution was obtained by autoclaving at 121 °C for 15 min.

2.1.2.6. Dey/Engley (D/E) Neutralizing Broth

Difco™ Dey/Engley (D/E) Neutralizing Broth (Becton, Dickinson & Company, USA) was prepared by adding 39 g of powder to 1 L of distilled water. Sterile solution was obtained by autoclaving at 121 °C for 15 min.

2.1.3. Plasma Equipment

The plasma system used for this research was from Plasmatreat USA Inc. (Elgin, IL, USA). Atmospheric pressure plasma was generated using the OPENAIR® PLASMA JET TECHNOLOGY, established by Plasmatreat. In this system, a high voltage between a stator and rotor allows generation of plasma within the nozzle, which is then discharged through the nozzle head using a working gas. A FG5001 Plasma Generator (Figure 9)

equipped with a RD1004 rotating nozzle (Figure 10) was used to generate the plasma. A rotating nozzle helps distribute the treatment evenly and is suited better to work with wider processing surfaces (Plasmatreat USA Inc., 2016). For this research, a voltage of 295 V, air pressure of 1990 mBar, and frequency of 22.5 kHz was employed to generate plasma. Figure 11 and Figure 12 show the actual and the schematic of setup of the plasma unit at Rutgers University, respectively, which was used for this research. Compressed, filtered, moisture free air was used as the feed gas.

Figure 9: Openair® FG 5001Plasma Generator (Plasmatreat USA Inc., 2016)

Figure 10: RD1004 rotating nozzle

Figure 11: Setup of plasma unit at Rutgers University: Air cylinder, air filter, generator, pressure regulator, and nozzle.

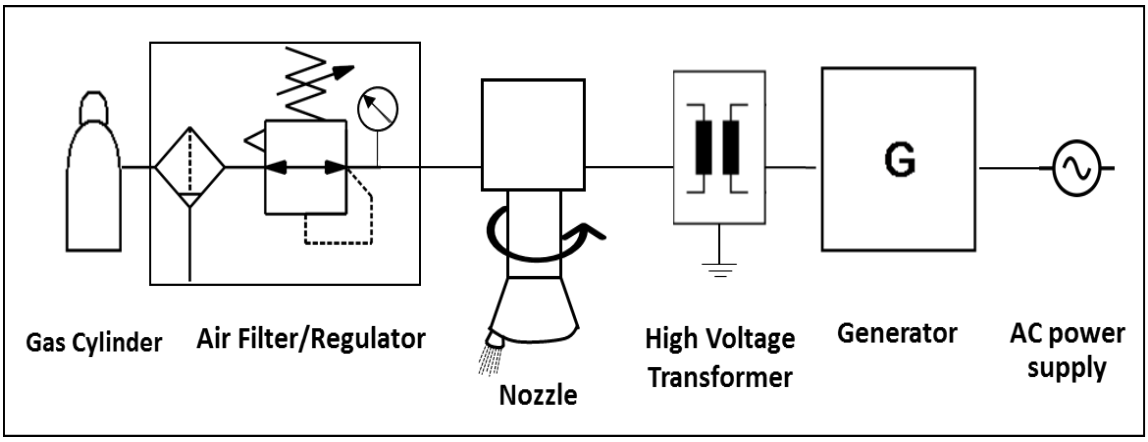

Figure 12: Schematic diagram of plasma unit set-up at Rutgers University.

The plasma unit was kept inside a fume hood to avoid any possible adverse reactions due to the reactive species generated, such as ozone or nitric oxide (NO_x) species.

2.1.4. Plasma Activated Water and Buffer

Distilled water was sterilized by autoclaving at 121 °C for 15 min to be used for generating plasma activated water (PAW). Citrate-phosphate buffer at pH 3.1, was prepared by mixing 4.29 g of sodium phosphate dibasic (Sigma Aldrich, USA) and 11.01 g of citric acid (Sigma Aldrich, USA) in a 500 ml volumetric flask and the volume was made up using distilled water. The pH of the prepared buffer was confirmed using an Orion Star™ A111 pH Benchtop Meter (ThermoFisher Scientific, USA) and a Orion™ 9157BNMD Triode™ 3-in-1 pH/ATC Probe (ThermoFisher Scientific, USA). The prepared buffer was then sterilized by autoclaving at 121 °C for 15 min. No significant change was observed in the pH of the buffer post autoclaving.

2.1.5. Hydrogen Peroxide Assay chemicals

The following solutions were prepared for the Hydrogen peroxide assay:

- ✓ Sulfuric acid (2 M) solution:

17.97 M sulfuric acid solution (95.8% pure Sulfuric acid, Sigma Aldrich, USA) was diluted with distilled water in appropriate proportions to obtain a 1 L solution of 2 M sulfuric acid.

- ✓ Titanium sulfate reagent:

25 g of Titanium oxysulfate (Sigma Aldrich, USA) was dissolved in 1 L of 2 M sulfuric acid (prepared as mentioned above) with constant stirring. The reagent was cooled and stored in cool, dark place in an amber colored bottle.

- ✓ Sodium azide reagent:

Sodium azide (Sigma Aldrich, USA) was dissolved in distilled water in appropriate proportions to prepare 60 mM solution of sodium azide.

Sodium azide is classified as H310 (fatal on skin contact), Dermatril™ Nitrile gloves, so, that have been tested for hand protection were used while handling the chemical.

- ✓ Hydrogen peroxide solutions for standard curve:

Hydrogen peroxide solution (30 wt. % in H_2O, ACS reagent) was obtained from Sigma Aldrich, USA. The reagent was diluted with distilled water to achieve the following concentrations: 5 µM, 10 µM, 15 µM, 25 µM, 50 µM, 100 µM, 250 µM, 500 µM, 750 µM, 1000 µM. The above solutions were used to generate a standard curve to estimate the concentration of hydrogen peroxide in sample systems using their absorbance values at 407 nm.

2.1.6. Fresh produce

Fresh produce samples were selected based on visual differences in their surface roughness, which was then quantified using a CLSM. Grape tomatoes, limes, kiwis,

peaches, apricots, strawberries, and spiny gourds were bought from a local supermarket, transported to laboratory and kept at 4 °C. Samples were always used within three days of purchase.

2.1.7. Instruments used in this study

- ✓ Black-Comet UV-VIS Spectrometer (StellarNet Inc., Tampa, USA) with a F400-UV–vis-SR fiber optic in the range from 190 nm to 850 nm and a collimating lens QCol for Optical Emission Spectroscopy.
- ✓ Orion Star™ A111 pH Benchtop Meter with an Orion™ Metallic Combination Electrode (9678BNWP) (Redox/ ORP model with Epoxy body) for Oxidation-Potential measurement.
- ✓ Orion Star™ A215 pH/Conductivity Benchtop Multiparameter Meter with an Orion™ DuraProbe™ 4-Electrode Conductivity Cells for Electrical Conductivity measurement.
- ✓ Epoch™ Microplate Spectrophotometer with a monochromator-base UV-Vis wavelength selection of 200 nm to 999 nm, a 6- to 384- microplate reading capability and operated by a Gen5 Data Analysis software interface.
- ✓ Zeiss 780 Laser Scanning Microscope (Oberkochen, Germany) with topography software as provided by Zeiss, based on the DIN EN ISO 4287.

2.2. Methods

2.2.1. Determining optimum distance between substrate and plasma nozzle, and time of exposure

Although the Plasmatreat system is used to generate cold atmospheric pressure plasma, the temperature of plasma inside and near the nozzle is high (~195 °C). Previous research done by Bhide (2016) in our lab, established that a working distance of 7.7 cm or higher between the substrate and plasma nozzle allows the plasma to cool down to a temperature of ≤ 50 °C. Bhide (2016) used an infrared temperature sensor to ensure that the temperature did not exceed 50 °C at the given working distance of 7.7 cm. The temperature limit was set based on preliminary experiments conducted by Bhide, (2016) to ensure that temperature (50 °C) had negligible or undetectable role in microbial inactivation studies for *Enterobacter aerogenes*.

Based on this knowledge, a working distance of 8.1 cm was used (≥7.7 cm) to ensure temperatures below ≤ 50 °C, during the generation of plasma activated water. Lower distances resulted higher temperatures of water leading to evaporative losses of the water exposed to plasma. Preliminary experiments conducted for different exposure times established that exposure of 200 ml of water to plasma for 5 min at a distance of 8.1 cm, helped maintain temperature of PAW to below 50 °C. The distance – temperature - time combination was selected such, to avoid loss of reactive species with increasing distance while maintaining the temperatures below 50 °C and avoiding any potential evaporative losses of water as well.

2.2.2. Plasma Activated water (PAW) and Plasma Activated Buffer (PAB) preparation

Plasma activated water (PAW) was generated by exposing 200 ml of sterilized distilled water in a 1000 ml Pyrex® glass beaker for 5 min. A distance of 8.1 cm was maintained between the surface of water and the plasma nozzle, to ensure that the temperature of water did not exceed 50 °C. On exposure of water to plasma for 5 min, pH of water dropped to 3.1 from initial pH of 6.5. Water temperature was measured to confirm that it was below 50 °C.

Plasma activated buffer (PAB) was prepared in a similar manner as plasma activated water. No significant pH drop from the initial pH of 3.1 was observed for the buffer when exposed to plasma.

2.2.3. Preparation of Overnight Bacterial Culture

Using a sterile loop, bacterial inoculum was retrieved from the frozen glycerol-culture stock (as explained in section 2.1.2.1), transferred to a sterile centrifuge tube containing 30 ml of Tryptic soy broth containing 50 µg/ml Nalidixic acid and incubated for 24 h at 37 °C. A loop of this culture was streaked for isolation onto a Tryptic Soy Agar petri plate containing 50 µg/ml Nalidixic acid. The plate was incubated for 24 h at 37 °C. A single colony retrieved from this plate was transferred to cultivate in a sterile centrifuge tube containing 30 ml of Tryptic soy broth (containing 50 µg/ml Nalidixic acid) and incubated for 24 h at 37 °C. The broth was then centrifuged (5000 g, 10 min, 4 °C) in a Sorvall™

Legend™ X1 Centrifuge (ThermoFisher Scientific, USA). The bacterial pellet was removed and re-suspended in 30 ml 0.1% peptone water. This was repeated twice. The bacterial pellet was finally re-suspended in 10 ml of 0.1% peptone water. This suspension was used for all subsequent inoculation procedures. Cell count was determined via serial dilutions of the suspension and subsequent enumeration on Tryptic Soy Agar (with nalidixic acid (50 µg/ml)) and was approximately 10^9 CFU/ml.

2.2.4. Preliminary Experiments with PAW and PAB with respect to time

Hundred microliters of *Enterobacter aerogenes* inoculum (10^9 CFU/ml) prepared as described above was transferred to sterile 1.5 ml Eppendorf tubes, containing 1 ml of,

a) Sterilized distilled water

b) Plasma activated water (prepared as per section 2.2.2)

c) Sterilized citrate-phosphate buffer solution at pH 3.1 (prepared as per section 2.1.4)

d) Plasma activated buffer (prepared as per section 2.2.2)

The bacterial inocula were held for zero min, 5 min and 10 min, where zero-min sample served as the control. At the end of each period, each sample was serially diluted in 0.1% peptone water and plated in duplicates on Tryptic Soy Agar plates (with 50 µg/ml Nalidixic acid). Plates were incubated for 24 h at 37 ˚C and enumerated. Reductions was expressed as change in log CFU/ml.

2.2.5. Characterization of Plasma, Plasma Activated Water and Plasma Activated Buffer

2.2.5.1. Optical Emission Spectroscopy

A Black-Comet UV-VIS Spectrometer (StellarNet Inc., Tampa, USA) was used identify and relatively quantify the reactive species concentration in the gas phase plasma jet system (in air) at a working distance of 8.1 cm in the axial direction (Surowsky et al., 2014). The UV-VIS Spectrometer was equipped with a F400-UV–vis-SR fiber optic probe to obtain measurements in the range 190 nm to 850 nm. Each measurement was performed three times with an integration time of 1 millisecond and with three scans per average. The spectral peaks obtained on the emission spectra were identified using the SpectraWiz® spectrometer software provided by StellarNet Inc., and National Institute of Standards and Technology for Atomic Spectra Database (Kramida, 2014).

2.2.5.2. Electrical Conductivity

Electrical conductivity was measured in micro-Siemens/cm (µS/cm) using an Orion Star™ A215 pH/Conductivity Benchtop Multiparameter Meter with an Orion™ DuraProbe™ 4-Electrode Conductivity Cells probe. The meter was calibrated using 5 µS/cm (R2236020) and 100 µS/cm (R2237000) conductivity standard solutions from Ricca Chemical Company, USA. The probe was immersed in the solutions to be quantified until a stable reading was obtained. Each solution was measured in triplicate and an average, standard deviation, and standard error were calculated.

2.2.5.3. Oxidation- Reduction potential

Oxidation- Reduction potential was measured in RmV (relative millivolts) using an Orion Star™ A111 pH Benchtop Meter with a 9678BNWP Orion™ Metallic Combination Electrode (Redox/ ORP model with Epoxy body) probe. A 4M KCl saturated with AgCl solution (900011) (ThermoFisher, USA) was used as the filling solution for the Sure-Flow™ ORP electrode. The electrode was standardized using an ORP standard solution (967901) (ThermoFisher, USA) and set to +220 mV. Readings were obtained in relative millivolts to calibrate the offset of the sample. The probe was immersed in the solutions to be quantified until a stable reading was obtained. Each solution was measured in triplicate and an average, standard deviation, and standard error were calculated.

2.2.5.4. Hydrogen Peroxide Assay

The following procedure is based on the method developed by Eisenberg in 1943 with modifications suggested by Graves 2013:

a. Transfer 100 µL of sample in 96 well-plate
b. Immediately add 10 µL of sodium azide (60 mM) solution per 100 µL of sample, if nitrites are expected to be present in the sample. Pipette the sample repeatedly to mix well.

c. Add 50 µL of prepared titanium sulfate reagent per 100 µL of sample in the 96 well-plate. (** If the sample contains peroxides, it will produce a yellow color**)
d. Measure the absorbance using a UV-Vis spectrophotometer (Epoch Microplate Spectrophotometer) (BioTek Instruments Inc., USA) at 407 nm.
e. Include an appropriate blank, to be subtracted from the sample absorbance readings.
f. Perform the measurements in triplicates.
g. Obtain a data fit (standard curve) using the hydrogen peroxide solutions of known concentrations. Calculate the correlation co-efficient to help find the amount of hydrogen peroxide in unknown samples.

2.2.6. Quantification of Surface Roughness using Confocal Laser Scanning Microscopy (CLSM)

Surface roughness for a glass slide, grape tomato, lime, kiwi, strawberry, peach, apricot, and spiny gourd was quantified using a Zeiss 780 Laser Scanning Microscope (Figure 13) (Oberkochen, Germany). The protocol established by Sheen et al. (2008), was slightly modified to obtain quantitative data for the roughness parameter 'P_q' for the samples to be tested.

Figure 13: Zeiss 780 Laser Scanning Microscope (Source: http://dm1084.wixsite.com/rutgersmicroscopy/confocal)

The skin of each fresh produce sample was peeled carefully. Care was taken to obtain samples as flat as possible, to avoid any added discrepancies in roughness measurement. A 1.0 cm x 1.0 cm square piece was cut and carefully pasted on a glass slide using a strong adhesive, as shown in Figure 14.

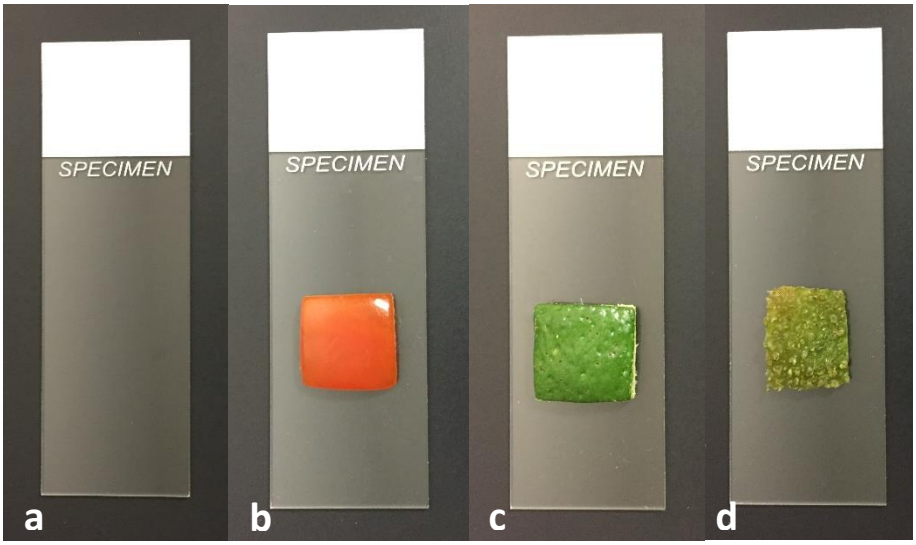

Figure 14: Samples ((a) glass slide, (b) grape tomato, (c) lime, (d) spiny gourd) prepared for surface roughness measurement using CLSM

Samples were mounted on the stage to be illuminated by a Diode 405-30 Laser at 405 nm using an inverted microscope. Reflection from sample surfaces was collected with a EC EpiIplan Apochromat 20X lens in a 16 bit channel and 1.00 P AU pinhole (26 µm); with image dimensions of 424.68 µm x 424.68 µm in the X-Y plane and dimensions for z-axis were set by using begin and end limits of the vertical series in the Z-wide scan control. A MBS T80/R20 beam splitter was used and each frame was 1024 x 1024 pixels. A zoom of 1.0 (default) was used and the master gain was adjusted for each sample to obtain maximum information. Image stacks with the optimal number of sections for maximal z-resolution (for the lens) were transformed into 3D images and topographical images. Roughness for each sample was quantified based on the DIN EN ISO 4287 using a Zeiss topography software.

Roughness was quantified for the primary profile, using the parameter, 'P_q', (as shown in Equation 2) which is the root mean square deviation of the assessed profile (ISO 4287-1997, (Mattsson et al., 2008; Standardization, 1997)).

$$P_q = \sqrt{\left(\frac{1}{L}\right) * \int_0^L z^2(x)dx} \qquad \text{(Equation 2)}$$

Where L is the evaluation length, z is profile height for each point (peak or valley) at every point (x). Unit for P_q is micrometers.

Roughness was quantified as 'P_{sq}', using the topography software, based on the entire region scanned and indicating multiple specific regions of interest based on line segments.

Three spots were randomly selected on one sample for each surface and three such samples were used, so the 'P_q' obtained was an average assessment of nine 'P_{sq}' values for each surface.

2.2.7. Microbiological Analysis in the Planktonic System

One hundred microliters of *Enterobacter aerogenes* inoculum prepared as mentioned above was transferred to sterile Whirl-Pak® bags to be treated with the sanitizing solutions. Each bag containing 200 ml of sanitizing solution (water, PAW, buffer, PAB), was placed in a 1-L Pyrex® beaker and agitated on a rotary shaker for 3 min at 50 rpm.

Samples were serially diluted in 0.1% peptone solution were plated in duplicates on Tryptic Soy Agar (with 50 µg/ml Nalidixic acid). Plates were incubated for 24 h at 37 ˚C and enumerated. Reductions were expressed as change in log CFU/ml.

2.2.8. Microbiological Analysis on Different Surfaces

Samples were spot inoculated with a 0.1 ml of *Enterobacter aerogenes* inoculum prepared as mentioned above. Care was taken to avoid inoculating the grape tomatoes on the stem scar end, since it has been suggested that the stem scar tissue is prone to microorganism infiltration. The procedure followed was referred from Lang et al., (2004). The inoculum was approximately equally distributed on the glass slide (2.5 cm x 2.5 cm) and the skin of the fruit to avoid drip and facilitate uniform inoculation at all locations. Spot inoculation allows application of consistent and known volume of inoculum, that facilitates determining the reduction in microbial population correlating it to the sanitizer efficacy.

The samples were dried in a biosafety hood for 2 h at (22 ± 2 ˚C) following the spot inoculation. The samples were transferred to sterile Whirl-Pak® bags to be treated with sanitizing solutions, after drying. Each bag was treated with 200 ml of water, PAW, buffer, or PAB, and placed in a 1-L Pyrex® beaker and agitated on an orbital shaker (Lab Line, India) for 3 min at 50 rpm at room temperature.

Each washed sample was aseptically transferred to a sterile bag using sterile mini tongs (Bel-Art, USA) and 20 ml of Dey-Engley neutralizing broth (DE broth, pH 7.6, Difco) was

immediately added to it. Each sample was gently massaged for 1 min to facilitate recovery.

Samples were serially diluted in 0.1% peptone solution and plated in duplicates on Tryptic Soy Agar (with 50 µg/ml Nalidixic acid). Plates were incubated for 24 h at 37 ˚C. The remaining D/E solution containing the treated sample was incubated with 100 ml of Tryptic Soy Broth (with 50 µg/ml Nalidixic acid) to test for any remaining bacteria on the sample.

Undiluted wash water samples were plated in duplicated on Tryptic Soy Agar (with 50 µg/ml Nalidixic acid) and incubated for 24 h at 37 ˚C. Inoculated samples without any sanitizing treatment, were also subjected to gentle massaging for 1 min in 20 ml of DE broth, and were regarded as control samples. These samples were also subjected to serial dilution in 0.1% peptone solution, followed by plating in duplicates on Tryptic Soy Agar (with 50 µg/ml Nalidixic acid) and incubated for 24 h at 37 ˚C. Experiments were performed in triplicates for each fruit treated with four sanitizing solutions and a control. Microbial inactivation was expressed as change in log CFU/surface. Microbial recoveries of approximately 7 log CFU/surface were attained from different surfaces from inoculation of approximately 8 log CFU/surface.

2.2.9. Storage Stability of PAW and PAB with respect to pH and ORP over Time

Stability of PAW and PAB was assessed over seven days by measuring temperature, ORP and pH. Parameters were measured for first six hours at hourly interval and daily after that. The flasks containing the PAW and PAB were kept covered using aluminum foil, to minimize air-water interactions.

2.2.10. Statistical Analysis

The data were subjected to statistical analysis using one way analysis of variance (ANOVA) in Microsoft® Excel® 2016. A significance level ($p < 0.05$) was used to assess if the differences within the means were statistically significant.

3. RESULTS AND DISCUSSION

3.1. Preliminary Results with PAW/ PAB with respect to time

Figure 15, represents the reductions in *E. aerogenes* obtained after treatment with sterile distilled water, PAW, buffer and PAB, for 5 and 10 min. The initial populations obtained, which served as control, were based on zero min of incubation of each solution with the bacteria. Treatment for 10 min showed significantly higher reduction than 5 min treatment for both, PAW and PAB. After 10 min, PAW (pH = 3.1) achieved (1.92 ± 1.58) log CFU/ml reduction, while buffer (at pH 3.1) and distilled water did not show any significant reductions which were (0.08 ± 0.18) log CFU/ml and (0.09 ± 0.17) log CFU/ml, respectively. These results suggested that the reduction obtained with PAW was due to the action of reactive species and not due the acidic pH alone. Moreover, on treatment for 10 min, PAB achieved a much higher reduction of (5.11 ± 1.40) log CFU/ml than PAW, suggesting an interactive effect of the existing low pH of the buffer and the plasma generated reactive species in the buffer. It may be hypothesized that certain secondary species may be developed due to multiple ionic reactions in PAB, that may contribute to the increased anti-microbial effect. The procedure followed had a detection limit of 2.74 log CFU/ml for microbial enumeration.

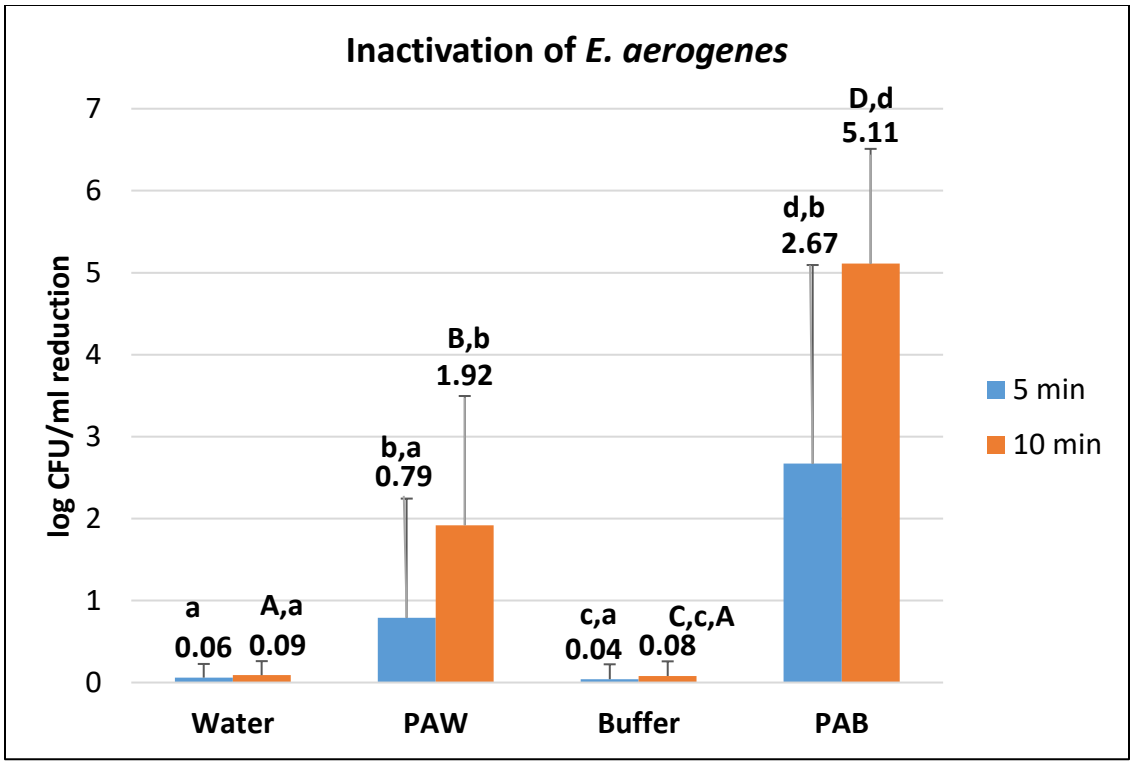

Figure 15: Inactivation of *Enterobacter aerogenes* in suspension after treatment with distilled water, PAW, Buffer, and PAB for 5 and 10 min. (Error bars indicate standard deviation; Data that do not share same letter (lowercase and uppercase), are significantly different from each other (One-way ANOVA, $p<0.05$)).

3.2. Characterizing Plasma, Plasma Activated Water and Plasma Activated Buffer

3.2.1. Optical Emission Spectroscopy

Figure 16, represents the optical emission spectra obtained for the plasma jet system at a working distance of 8.1 cm. Relative concentrations of oxygen and nitrogen ions were recorded with the emission spectrum in gas phase and not in liquid systems. Atomic

Spectra Database from the National Institute of Standards and Technology (Kramida, 2014) was used to identify the peaks obtained in the spectra based on their observed wavelengths.

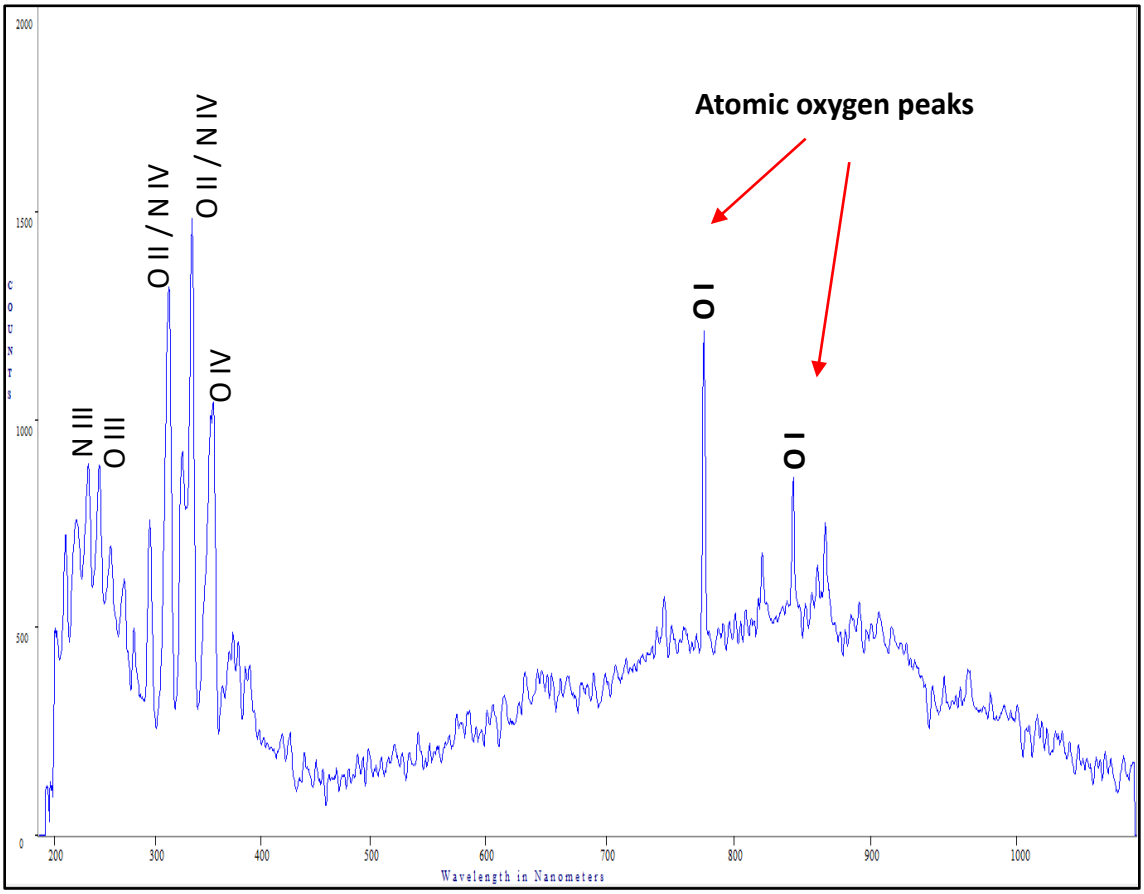

Figure 16: Emission spectra recorded for the air plasma jet system at a distance of 8.1 cm from the nozzle using OES

Strong atomic oxygen peaks were observed at 777 nm and 844 nm. Previously, researchers (Ma et al., 2015; Tian et al., 2015; Zhang et al., 2013) have reported that

these peaks correspond to oxygen atom transitions, O (3p5P→3s5S) at 777 nm and O (3p3P→3s3S) at 844 nm. Excited atomic species produced above the surface of water (such as hydroxyl radical (•OH), singlet oxygen ($^1O_2$), and superoxide anion ($^{\bullet}O_2^-$)), may be diffused into the liquid to generate other reactive oxygen species, such as hydrogen peroxide (H_2O_2) (Ma et al., 2015). Dissociated water molecules formed due to plasma attribute to the OH band observed at 306 nm - 315 nm (Tatarova et al., 2010; Tian et al., 2015). Reactive oxygen and nitrogen species such as atomic oxygen (O), ozone (O_3), hydroxyl ion (OH•), NO, NO_2, are generated in air plasma and are known to have direct impact on microorganism cell. They attack the unsaturated fatty acids present in the lipid bilayers in the outer cell membrane of the microorganism, leading to compromised cell integrity and eventually cell death. These species also oxidize the amino acids, leading to microbial injury or death (Misra et al., 2011; Laroussi and Leipold, 2004).

3.2.2. Electrical Conductivity

Table 3, represents the electrical conductivity (µS) values measured with the Orion™ DuraProbe™ 4-Electrode Conductivity Cells probe for sterilized distilled water, PAW, sterilized buffer, and PAB solutions.

Table 3: Electrical conductivity values measured in (µS/cm) for distilled water, Plasma activated water, buffer and Plasma activated buffer (Data that do not share the same letter, are significantly different from each other (One-way ANOVA, $p<0.05$))

Distilled Water (µS/cm)	**PAW (µS/cm)**	**Buffer (µS/cm)**	**PAB (µS/cm)**
17.92 ± 2.36^{a}	324.19 ± 16.99^{b}	7820 ± 60.0^{c}	8690 ± 30.0^{d}

Plasma activation results in generation of ions in water. Electrical conductivity measurements for PAW reported previously (Ma et al., 2015; Xu et al., 2016) support the presence of active ions in the plasma treated solutions. Upon exposure of water and buffer to plasma to generate PAW and PAB, respectively, an increase in the electrical conductivity was observed for each solution. Greater increases in conductivity observed in the buffer solution compared to water may be attributed to presence of a weak acid and conjugate base and their ionic equilibria. The higher microbial inactivation efficacy observed for PAW and PAB as compared to distilled water and buffer (Figure 15), maybe attributed to the higher electrical conductivity values (Table 3), suggesting accumulation of ions in the solution (Tian et al., 2015).

3.2.3. Oxidation Reduction Potential

Table 4, represents the oxidation-reduction potential (RmV) values measured with the Orion™ Metallic Combination Electrode (Redox/ ORP model with Epoxy body) probe for sterilized distilled water, PAW, sterilized buffer, and PAB solutions.

Table 4: Oxidation-reduction potential values measured in relative millivolts (RmV) for distilled water, Plasma activated water, buffer and Plasma activated buffer ((Data that do not share the same letter, are significantly different from each other (One-way ANOVA, $p<0.05$))

Water (RmV)	**PAW (RmV)**	**Buffer (RmV)**	**PAB (RmV)**
376.54 ± 6.83^{a}	534.52 ± 5.97^{b}	511.06 ± 3.69^{c}	556.00 ± 2.25^{d}

The concentration of the oxidizers in a solution and their strength is indicated by the Oxidation-Reduction potential values of the solution (McPherson, 1993). ORP value is used to evaluate the global level of reactive oxygen species, which are known to have antimicrobial effect (Tian et al., 2015; Xu et al., 2016; Jin et al., 2016).

In a healthy cell, over 90% of glutathione exists in a reduced form of glutathione (GSH) (Halprin et al., 1967). In presence of oxidative stress environment, GSH is oxidized and converted to glutathione disulfide (GSSG). This change in the ratio of [GSH]/[GSSG], would result in a higher potential due to change in the redox state (Schafer et al., 2001). Liao et al. (2006), proposed that this change in redox state would affect and damage the inner and outer membranes of the microorganism leading to cell necrosis.

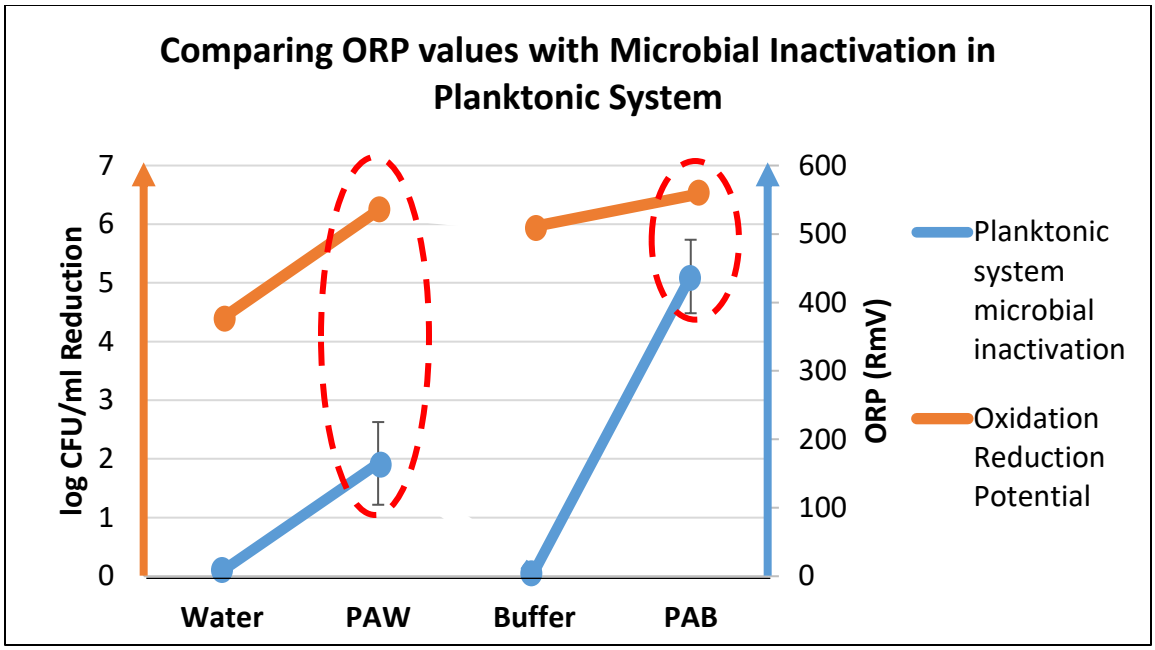

Figure 17: Comparison of oxidation- reduction potential measurements against inactivation of *Enterobacter aerogenes* in suspension after treatment with distilled water, PAW, Buffer and PAB for 10 min

Inactivation of *E. aerogenes* shown in Figure 15, is supported by the trend observed in the ORP values, as shown in Figure 17. Higher ORP values observed for PAW and PAB, may help to corroborate the higher kill achieved with PAW and PAB over time as explained in section 3.1. Thus, ORP serves as a good indicator for the efficacy of PAW and its antimicrobial capacity.

3.2.4. Hydrogen Peroxide assay

Following the Eisenberg (1943) protocol as mentioned in section 2.2.5.4, a standard curve for known concentrations of hydrogen peroxide (5 µM, 10 µM, 15 µM, 25 µM, 50 µM, 100 µM, 250 µM, 500 µM, 750 µM, 1000 µM) was obtained (Figure 18). Distilled water was used as a blank.

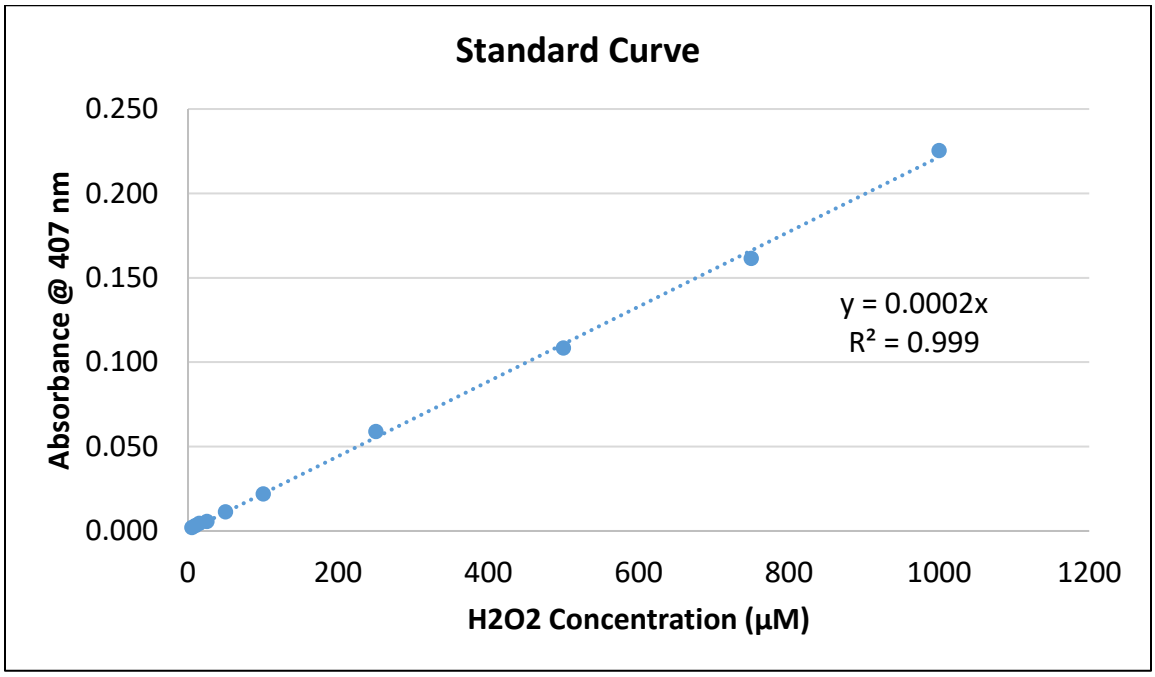

Figure 18: Standard curve for relating absorbance (at 407 nm) with known concentrations of hydrogen peroxide measured using a spectrophotometer

Increasing intensity of yellow color (higher absorbance at 407 nm) denoting an increase in the concentration of hydrogen peroxide is shown in Figure 19.

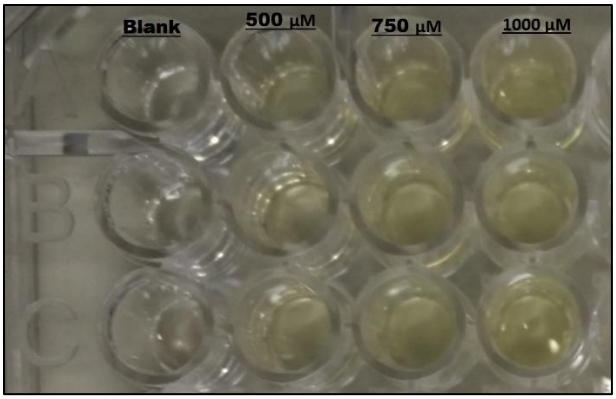

Figure 19: Intensity of yellow color observed with increasing concentrations of hydrogen peroxide (0 µM, 500 µM, 750 µM and 1000 µM) (three replicates are shown in the three rows)

Using the calibration equation thus obtained from the standard curve, the amounts of hydrogen peroxide in PAW, buffer, and PAB were estimated. No hydrogen peroxide was detected in either PAW or PAB, and while buffer and PAB, showed an increase in absorbance (data not shown), it was not due to an increase in yellow color obtained by the reaction between hydrogen peroxide and titanium oxysulfate reagent, but due to a non-yellow increase in turbidity as shown in Figure 20.

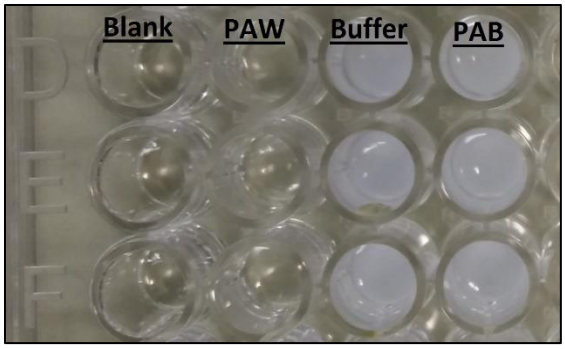

Figure 20: Turbidity observed in the buffer and the PAB samples on reaction with titanium oxysulfate

Previously, researchers have observed that the production rate of hydrogen peroxide is inversely correlated with the conductivity of solution for water treated with pulsed corona discharge and the authors attributed this to the hydrogen peroxide photolysis due to increasing UV radiation from the discharge with increasing conductivity (Lukes et al., 2008; Kirkpatrick et al., 2005). This may help explain the absence of hydrogen peroxide in the plasma activated water and plasma activated buffer, in the system.

3.3. Quantification of surface roughness using Confocal Laser Scanning Microscopy (CLSM)

Figure 21 illustrates the 3D topographical images of different samples along with the image of each surface. The 3D image allows for visual assessment for textural characteristics for each sample.

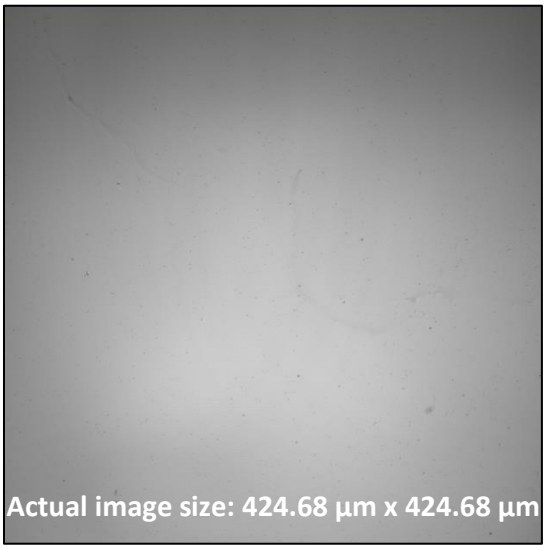

(a) Glass slide

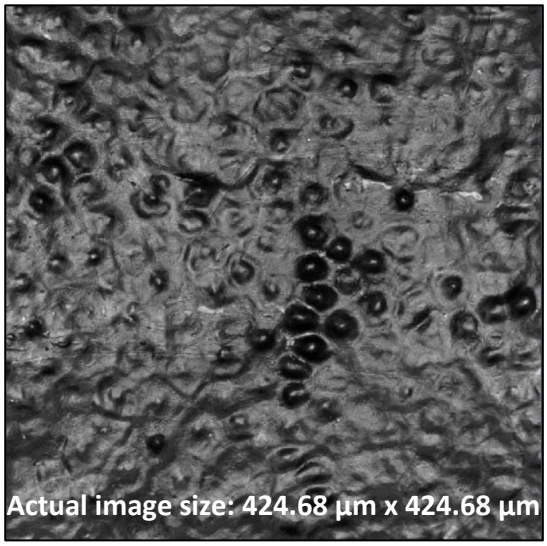

(b) Grape Tomato (Image source: Fresh Pac)

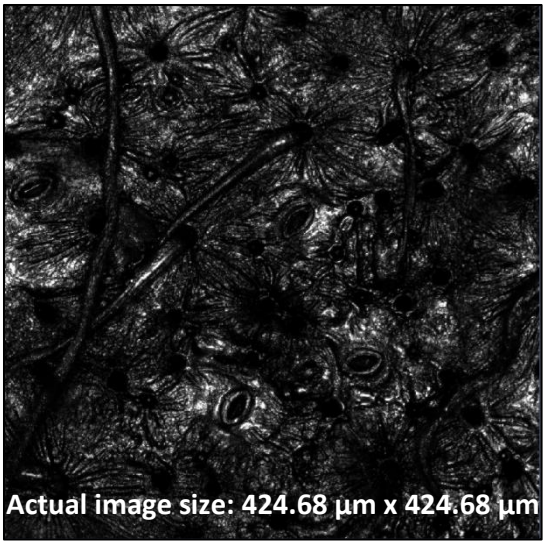

(c) Apricot (Image Source: Divine Organics)

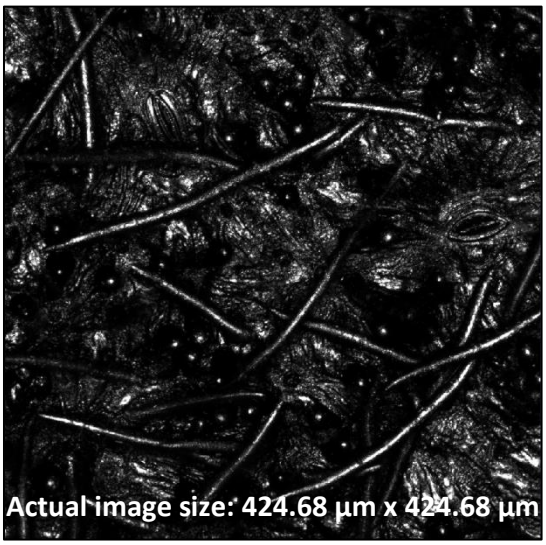

(d) Peach (Image Source: Weigh and Win)

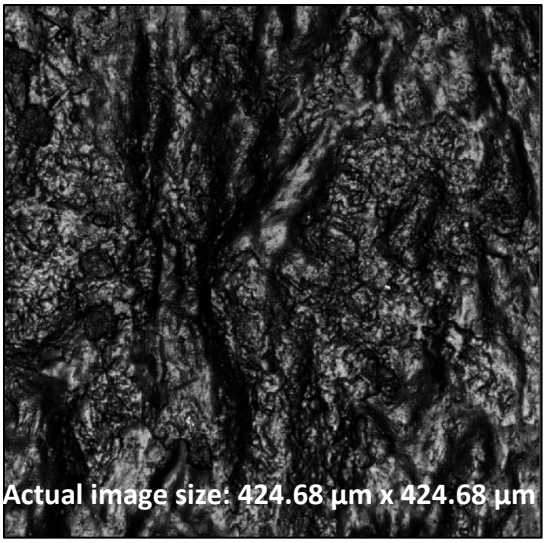

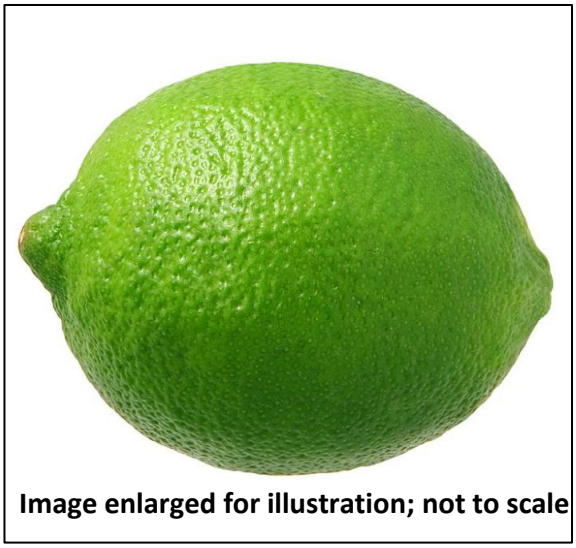

(e) Lime (Image Source: Giant Bomb)

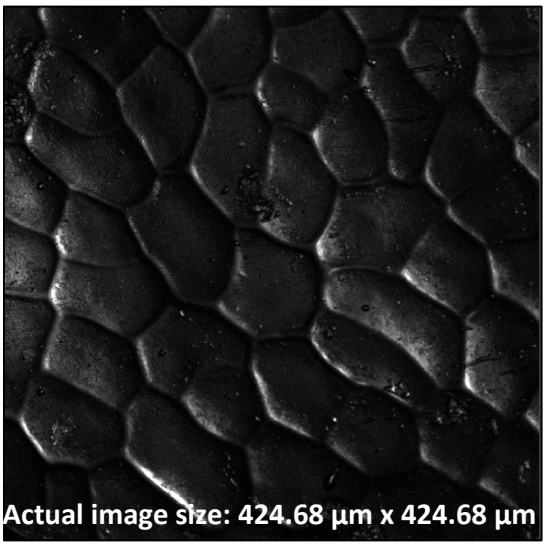

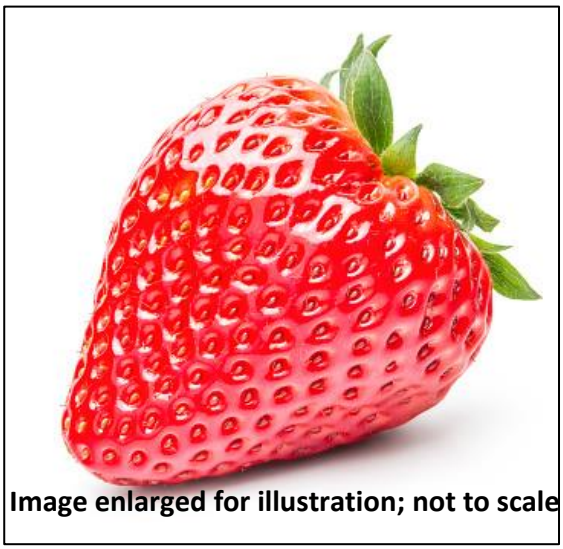

(f) Strawberry (Image Source: www.istockphoto.com)

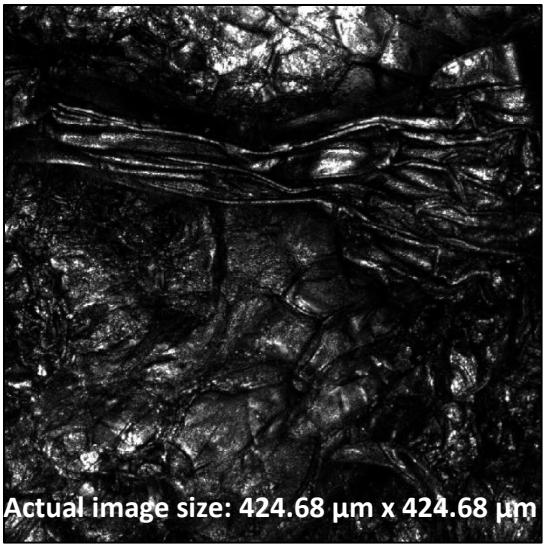

(g) Kiwi (Image Source: Pixabay)

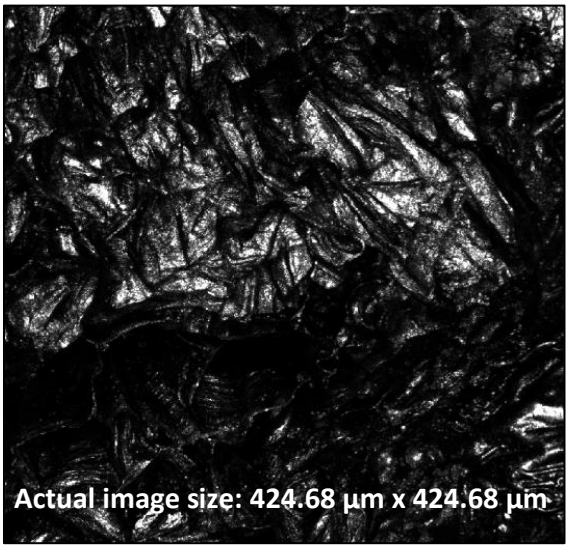

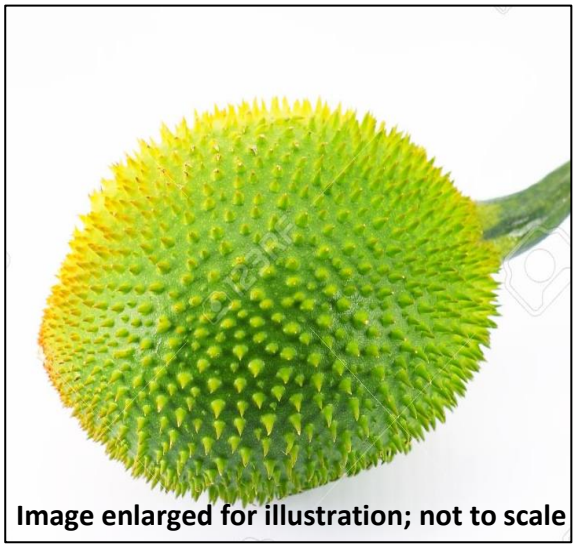

(h) Spiny Gourd (Image Source: 123RF.com)

Figure 21: 3D topographical images (left) and image of each surface (right) of (a) Glass slide, (b) Grape Tomato, (c) Apricot, (d) Peach, (e) Limes, (f) Strawberry, (g) Kiwi fruit, and (h) Spiny Gourd

The surface roughness P_q values quantified using equation 2 for each system are given in Table 5:

Table 5: Surface roughness measurements for different surfaces

Sample	**Surface Roughness (µm)**
Glass slide	0.28 ± 0.02[a]
Grape Tomatoes	5.17 ± 0.53 [b]
Apricots	17.55 ± 2.63 [c]
Limes	18.76 ± 3.00 [c]
Strawberry	22.48 ± 3.15 [c]
Peaches	23.97 ± 5.17 [c]
Kiwis	33.88 ± 9.73 [c]
Spiny Gourd	101.5 ± 10.95 [d]

((Data that do not share the same letter, are significantly different from each other (One-way ANOVA, $p<0.05$), n = 9)

Roughness values for the glass slide and grape tomatoes were significantly different ($p< 0.05$) from one other, however, apricots, limes, peaches, strawberries and kiwis did not significantly different roughness values from one another. Spiny gourds had a surface roughness significantly different from all other surfaces. The four surfaces chosen for

further microbiological experiments were glass slides, grape tomatoes, limes, and spiny gourds, the roughness values for which are shown in Figure 22.

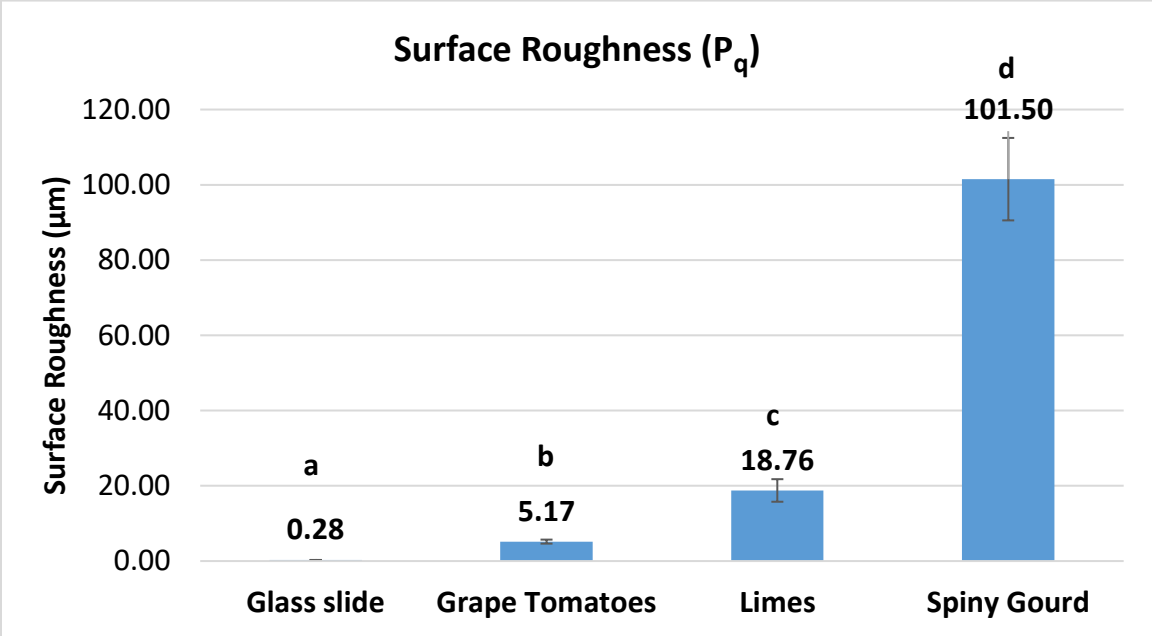

Figure 22: Surface roughness of samples selected for microbiological analysis (Error bars indicate standard deviation; Data that do not share the same letter, are significantly different from each other (One-way ANOVA, $p<0.05$))

3.4. Microbial inactivation obtained in planktonic system

Figure 23 represents data obtained for microbial inactivation of *E. aerogenes* in a planktonic system. As reported in section 3.1, distilled water treatment did not show any reduction (0.0 ± 0.02 log CFU/ml), while PAW achieved a reduction of (1.05 ± 0.12 log CFU/ml). No reduction (0.0 ± 0.05 log CFU/ml) was observed on treatment with

citrate-phosphate buffer of pH 3.1. Plasma activated buffer achieved a much higher log reduction (3.60 ± 0.70 log CFU/ml).

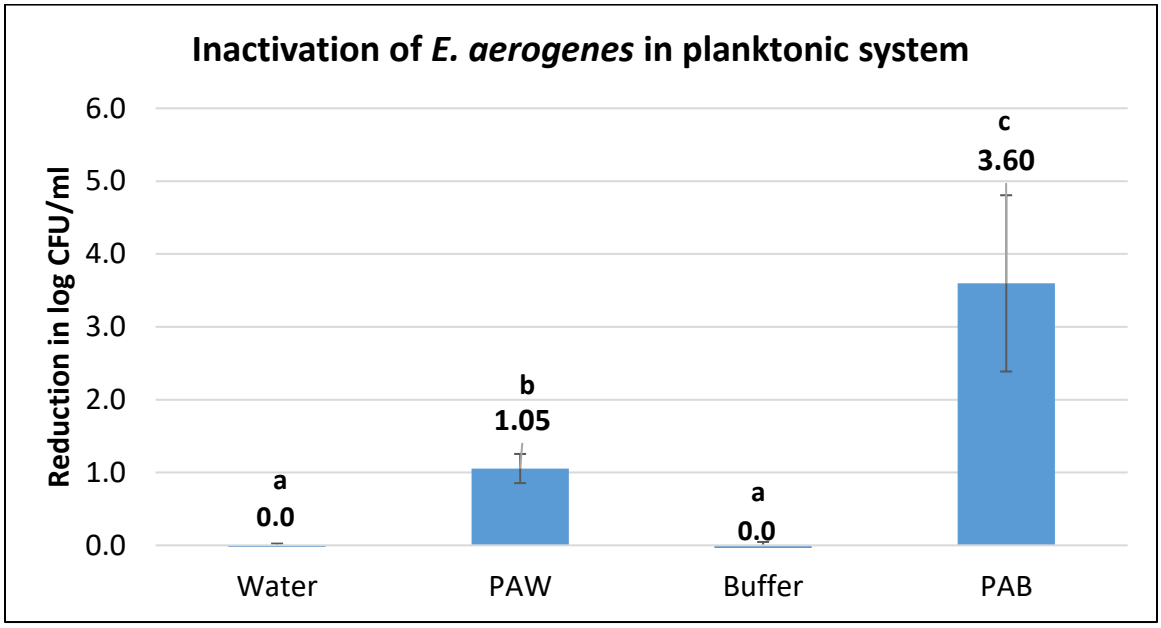

Figure 23: Inactivation of *Enterobacter aerogenes* on treatment with distilled water, PAW, Buffer, and PAB in planktonic system. (Error bars indicate standard deviation; Data that do not share the same letter, are significantly different from each other (One-way ANOVA, $p<0.05$))

The results obtained showed a similar trend to that reported in section 3.1, with no reduction obtained in the buffer only system, confirming that the inactivation of *E. aerogenes* was because of presence of reactive species and not acidic pH alone. Figure 23 also shows a significantly higher reduction obtained with PAB, as shown in section 3.1, correlated with a low pH and the likely presence of reactive species in PAB. The

procedure followed had a higher detection limit of 4.0 log CFU/ml for microbial enumeration owing to the higher volume of liquid used.

3.5. Microbial inactivation achieved on different surfaces

Figure 24 illustrates the reduction of *E. aerogenes* on different surfaces such as glass slide, grape tomatoes, limes, and spiny gourds, achieved with water and PAW.

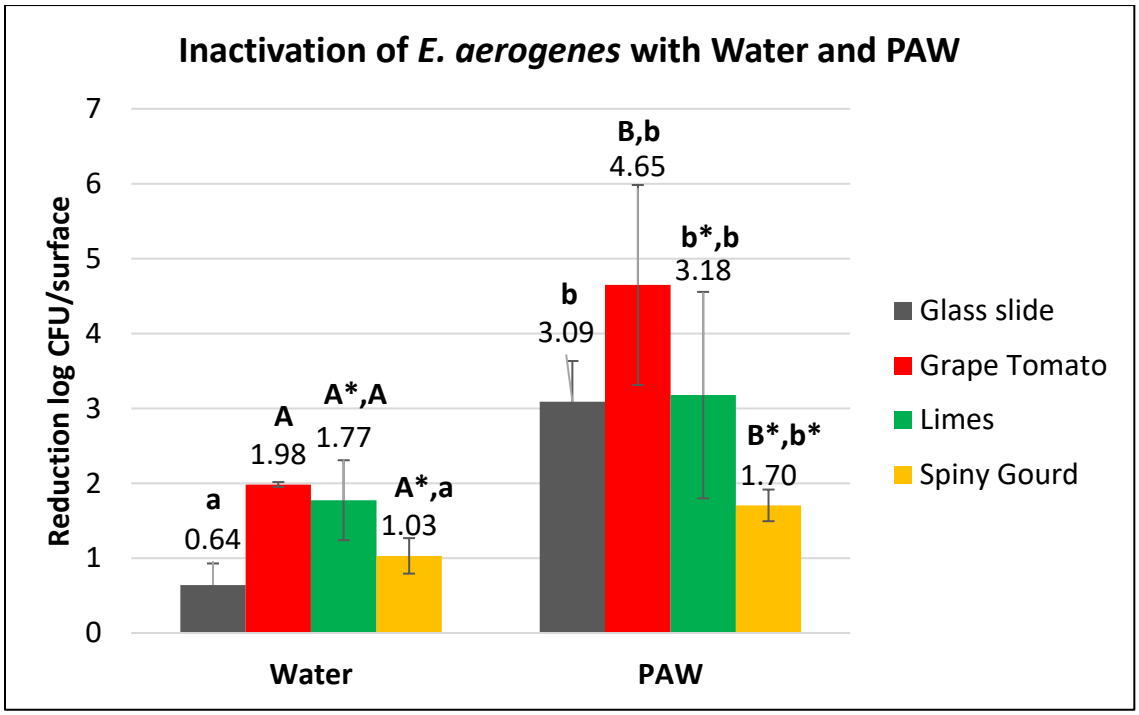

Figure 24: Inactivation of *Enterobacter aerogenes* on different surfaces of increasing roughness when treated with water and plasma activated water (Error bars indicate standard deviation; Data that do not share the same letter (uppercase and lowercase) with or without asterisks, are significantly different from each other (One-way ANOVA, $p<0.05$))

Unlike the planktonic system (described in section 3.4), reduction in *E. aerogenes* concentration was observed for all surfaces when treated with sterilized distilled water. The reduction on glass slide (0.64 ± 0.29 log CFU/surface) was significantly lower than on grape tomatoes (1.98 ± 0.03 log CFU/surface) and limes (1.77 ± 0.53 log CFU/surface). The reduction on glass slide was not significantly different than obtained on spiny gourd (1.03 ± 0.24 log CFU/surface). However, there was no significant difference in the reduction on grape tomatoes and limes, and limes and spiny gourd. To further investigate if this reduction was an effect of agitation during washing of each surface (detachment of bacteria from the surface), wash water was enumerated on TSA plates (as explained in section 3.6). This would help to asses if bacteria were inactivated by distilled water or just detached into wash water.

Significantly higher reductions in surface populations were observed when these surfaces were treated with PAW vs. distilled water. No significant difference was observed in bacterial reductions between glass slides (3.09 ± 0.54 log CFU/surface), grape tomatoes (4.65 ± 1.34 log CFU/surface) and limes (3.18 ± 1.38 log CFU/surface). Significantly lower reduction was observed on spiny gourds ((1.70 ± 0.21) log CFU/surface) than glass slide and grape tomatoes. These inconsistencies may be attributed to the high variability observed in the microbial reductions achieved with PAW for different surfaces. Effect of reactive species and washing (detachment of bacteria from surface) can be confirmed by evaluating the data obtained from wash water. The procedure followed had a detection limit of 2.0 log CFU/surface for microbial enumeration.

Figure 25 illustrates the reduction in *E. aerogenes* on glass slides, grape tomatoes, limes, and spiny gourds, achieved with buffer and PAB.

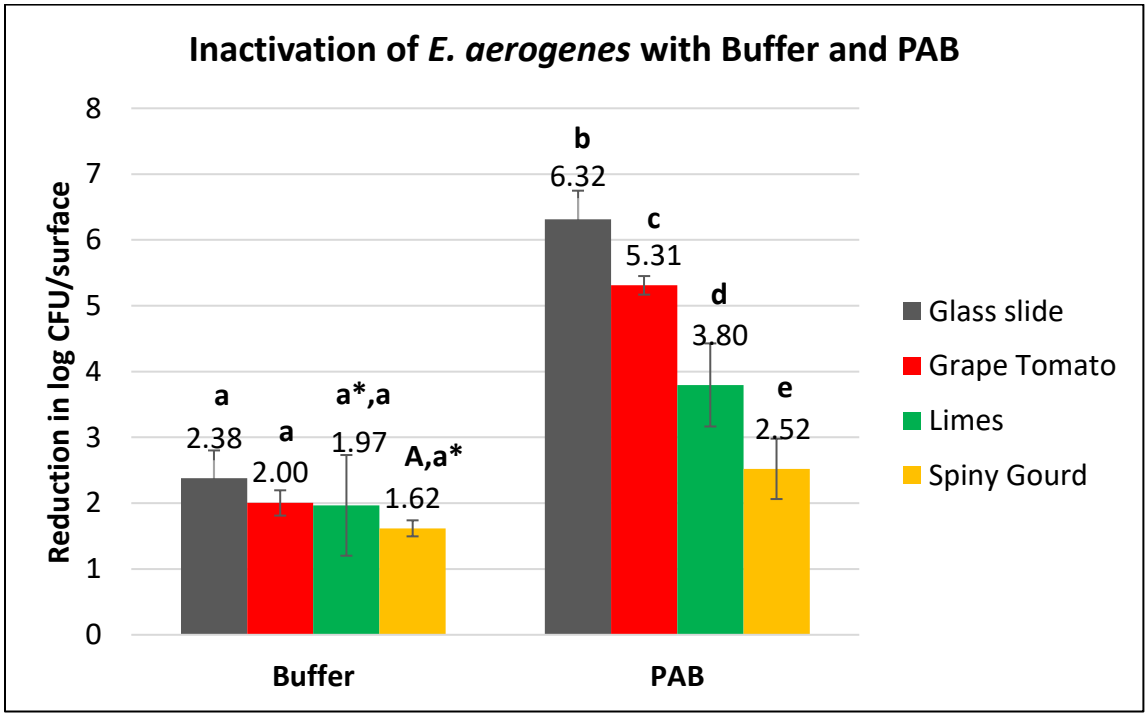

Figure 25: Inactivation of *Enterobacter aerogenes* on surfaces of increasing roughness when treated with buffer and plasma activated buffer (Error bars indicate standard deviation; Data that do not share the same letter (uppercase and lowercase), with or without asterisks, are significantly different from each other (One-way ANOVA, $p<0.05$))

The reduction in *E. aerogenes* concentration on glass slide (2.38 ± 0.42 log CFU/surface), grape tomatoes (2.00 ± 0.19 log CFU/surface), and limes (1.97 ± 0.77 log CFU/surface), achieved by washing with buffer was not significantly different. Buffer was significantly less effective in removing *E. aerogenes* from spiny gourds (1.62 ± 0.12 log CFU/surface) than from glass slides and grape tomatoes.

A significantly higher reduction in *E. aerogenes* concentration was observed when these surfaces (glass slide, grape tomatoes, limes and spiny gourds) were treated with PAB. As the surface roughness increased from glass slides (P_q = 0.28 ± 0.02) to grape tomatoes (P_q = 5.17 ± 0.53) to limes (P_q = 18.76 ± 3.00) to spiny gourds (P_q = 101.5 ± 10.95), significantly lower reductions were observed on glass slides (6.32 ± 0.43 log CFU/surface), grape tomatoes (5.31 ± 0.14 log CFU/surface), limes (3.80 ± 0.63 log CFU/surface), and spiny gourd (2.52 ± 0.46 log CFU/surface). Thus, surface roughness appears to play a significant role in the efficacy of PAB for washing fresh produce. Increasing surface roughness was correlated with lower microbial reductions achieved on each surface.

Figure 26 represents the summary of microbial reduction obtained for all surfaces of increasing roughness, i.e., a glass slide, grape tomatoes, limes, and spiny gourd, when treated with distilled water, PAW, buffer and PAB for 3 min with agitation at 50 rpm (as explained in section 2.2.8).

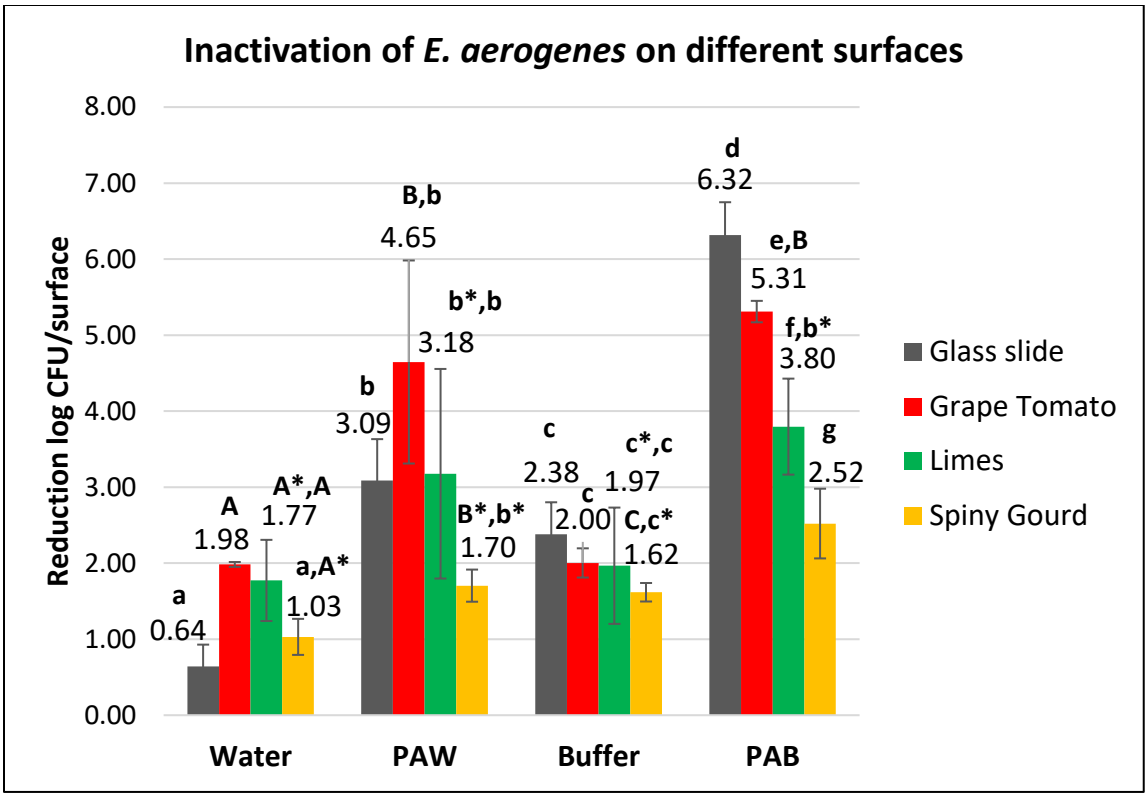

Figure 26: Inactivation of *Enterobacter aerogenes* achieved on different surfaces of increasing roughness when treated with water, plasma activated water, buffer and plasma activated buffer (Error bars indicate standard deviation; Data that do not share the same letter (uppercase and lowercase), with or without asterisks, are significantly different from each other (One-way ANOVA, $p<0.05$))

The inconsistency between the microbial reductions achieved with PAW and PAB for surfaces with increasing roughness values, may be attributed to the high variability in the microbial inactivation observed for different surfaces. A lower reduction was achieved for PAW for all surfaces, as compared to PAB. Thus, PAB proved to be a more effective sanitizer than PAW, that can achieve higher microbial reductions for smoother

surfaces, and but is affected by surface roughness, while still achieving higher microbial reductions than PAW.

3.6. Data obtained on wash water enumeration

In order to explain microbial reductions observed in section 3.5 using sterilized distilled water, PAW, buffer, and PAB, bacterial populations from wash water were enumerated to account for the detachment of bacteria (washing effect due to agitation provided) and to evaluate the effect of reactive species in PAW and PAB.

Figure 27 represents the wash water recovery data obtained for *E. aerogenes*, from water, PAW, buffer, and PAB, after the solutions were used to treat inoculated surfaces such as a glass slide, grape tomatoes, limes, and spiny gourds.

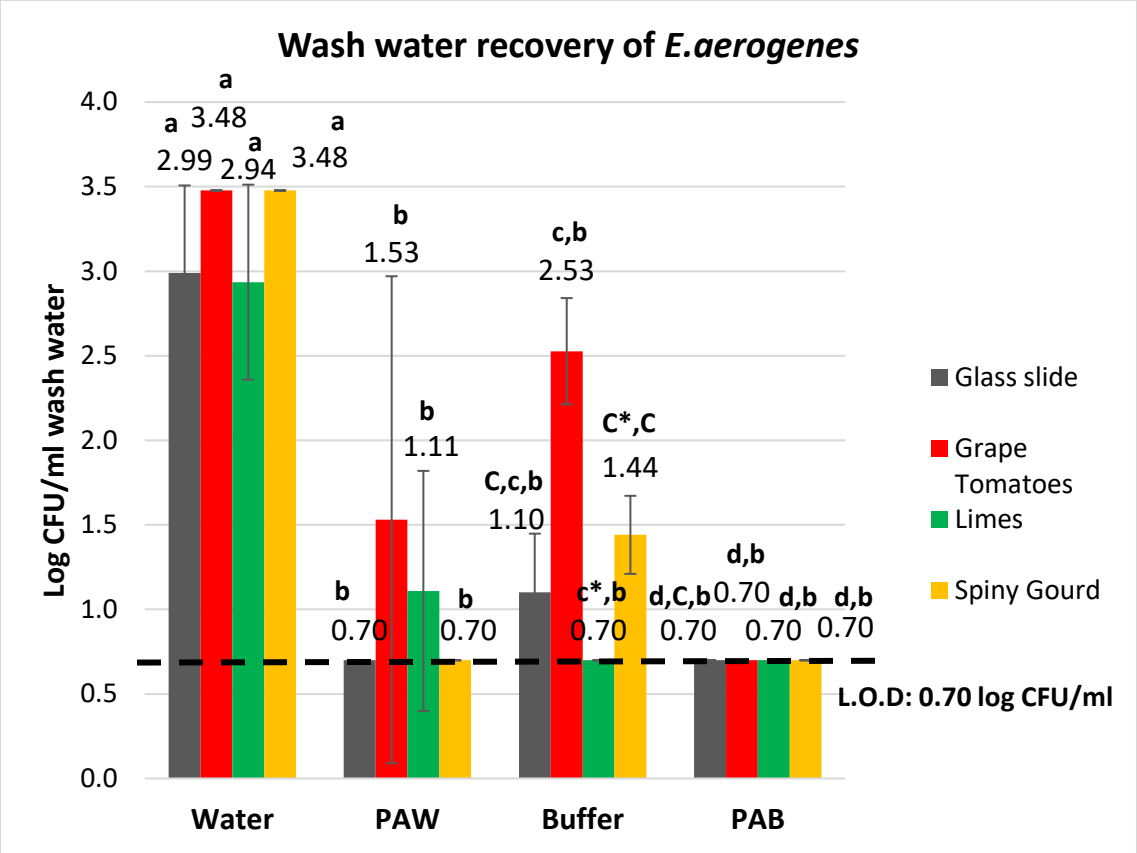

Figure 27: Recovery of *Enterobacter aerogenes* from distilled water, PAW, buffer, and PAB used for sanitizing surfaces with different roughness values (Vertical bars indicate standard deviation; Data that do not share the same letter (uppercase and lowercase), with or without asterisks, are significantly different from each other (One-way ANOVA, $p<0.05$)).

High concentrations of *E. aerogenes* were recovered from plain water used to wash glass slides (2.99 ± 0.52 log CFU/ml), grape tomatoes (3.48 ± 0.0 log CFU/ml), limes (2.94 ± 0.58 log CFU/ml), and spiny gourd (3.48 ± 0.0 log CFU/ml). *E. aerogenes* were recovered from the buffer solution (1.10 ± 0.35 log CFU/ml, 2.53 ± 0.31 log CFU/ml, 1.44

± 0.23 log CFU/ml) used to was for a glass slide, grape tomatoes, and spiny gourd, respectively, but were not recovered from buffer used to wash limes.

No *E. aerogenes* were recovered from PAB solutions, used to wash any surfaces, i.e., samples were always below detection limit (0.70 log CFU/ml). Recovery of *E. aerogenes* from PAW were possible in two cases, (1.53 ± 1.44 log CFU/ml, and 1.11 ± 0.71 log CFU/ml, for grape tomatoes, and limes, respectively) but was below the detection limit for glass slides and spiny gourds.

Higher populations of bacteria recovered from wash water solutions for distilled water and buffer suggest that bacterial reductions observed in section 3.5 with sterilized distilled water and buffer, may be an effect of detachment of bacteria (due to agitation during washing) from different surfaces into the water or buffer and not inactivation of *E. aerogenes*. Whereas, higher inactivation of *E. aerogenes* observed with PAW and PAB (as explained in section 3.5) and lower recovery of bacteria from plasma treated wash solutions, may be attributed to the presence of reactive species in PAW and not simply detachment of bacteria in to wash water solutions.

Infiltration of wash water contaminated with microorganisms into intercellular spaces of fresh produce has been reported previously (Gil, 2011). Usually the uptake of water by cellular pores is inhibited by internal gas pressure and surface hydrophobicity of the produce. However, higher produce temperature than wash, may affect pressure difference, leading to drawing of water by produce (FDA, 2015a). Additionally, washing of fresh produce with inadequately contaminated wash water may further lead cross

contamination (Danyluk and Schaffner, 2011). The integrity of wash water sanitizing solution important for both these reasons.

The generally lower recovery of *E. aerogenes* from plasma treated wash solutions indicate the potential of these solutions to be used for fresh produce in a dump tank washing process.

3.7. Storage Stability of PAW and PAB with respect to pH and ORP over Time

To assess the suitability of PAW and PAB as an industrial fresh produce sanitizer, it would be important to study their storage stability. In this study, the storage stability of PAW and PAB was evaluated over a period of seven days with respect to pH and ORP values.

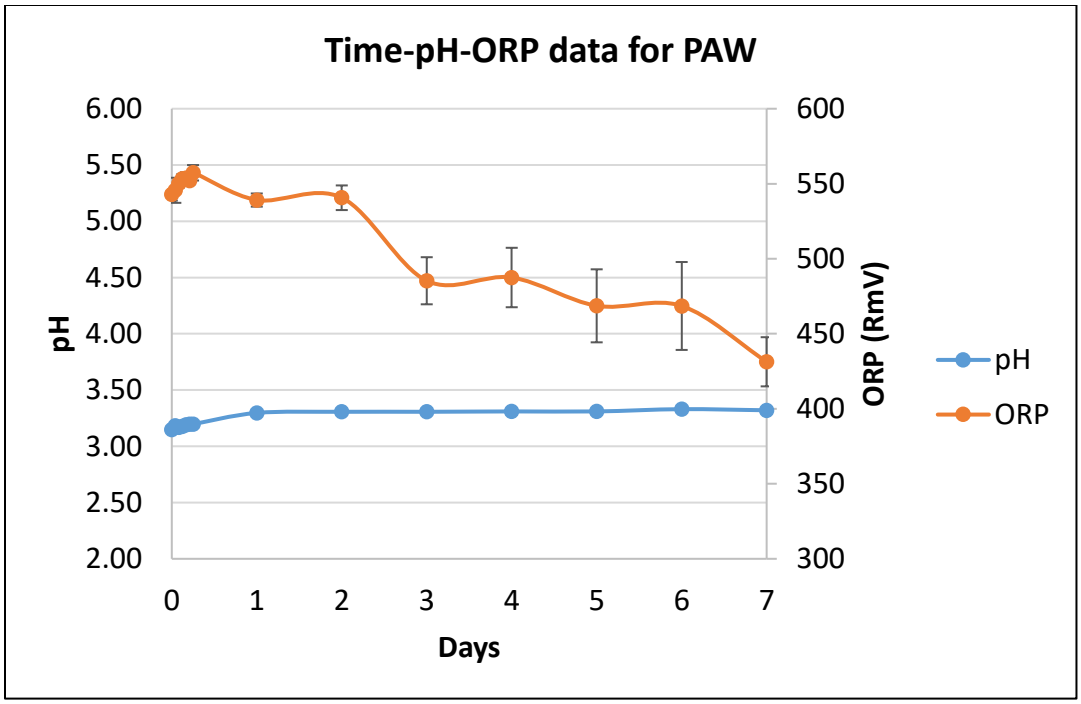

Figure 28: Storage stability of PAW for seven days, with respect to pH and ORP at room temperature (Error bars indicate standard error (n=3))

As shown in Figure 28, the pH of PAW remained stable over a period of seven days at room temperature. However, the ORP of PAW values exhibited a significant drop from day zero to day seven. With the apparent correlation between microbial inactivation and ORP values (reported in section 3.2.3), the ORP drop observed in Figure 28, may result in reduced efficacy for microbial inactivation. Further studies are required to confirm and quantify this effect.

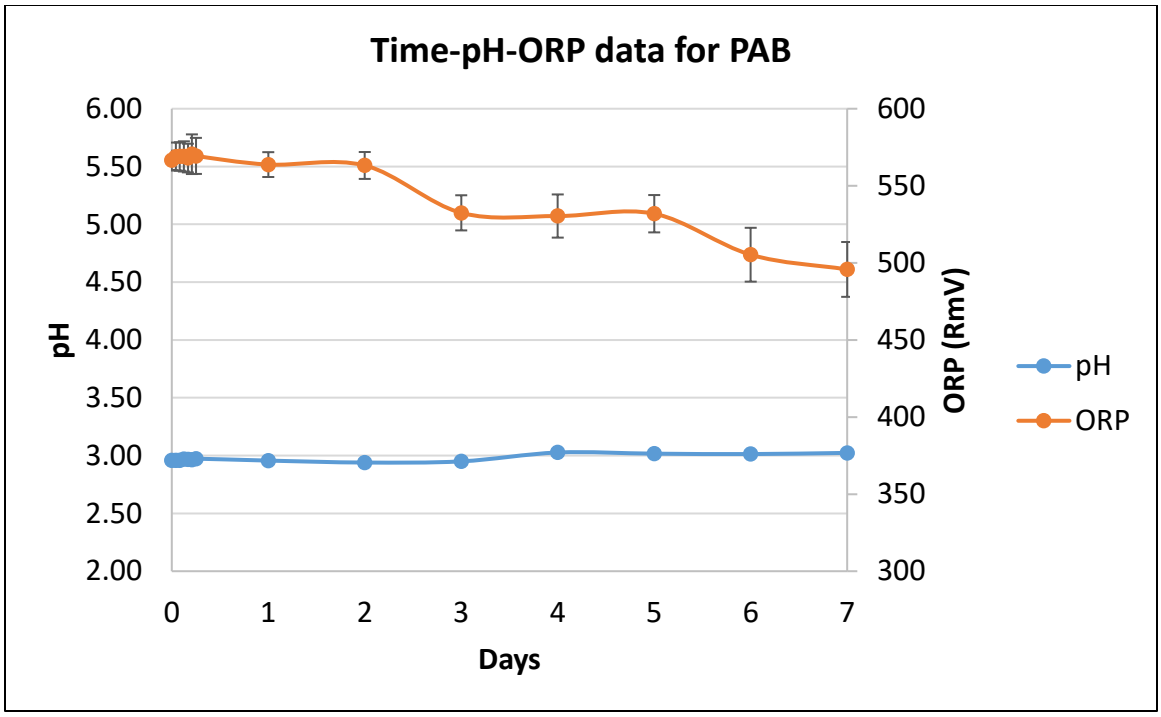

Figure 29: Storage stability of PAB for seven days, with respect to pH and ORP at room temperature (Error bars indicate standard error (n=3))

The pH of PAB remains stable over a period of seven days (Figure 29), while a decrease in ORP was observed, similar to that seen for PAW. The stability study for PAW and PAB show similar trends, and may provide useful insight for applications of PAW and PAB as industrial sanitizers.

4. CONCLUSIONS

Results with PAW and buffer in the planktonic system suggested that the microbial inactivation efficacy of PAW was not due to the acidic pH, but is likely due to the reactive species generated in the plasma treated liquid. Microbial inactivation achieved with PAB further suggested an interactive effect of low pH and reactive species in PAB. Further research to identify the active ions and species in PAB would provide greater clarity in determining the mechanism of PAB that explains microbial inactivation.

Characterization of plasma using OES helped identify reactive species in plasma, that have been reported to have antimicrobial effect. Moreover, electrical conductivity and oxidation reduction potential measurements for PAW and PAB confirmed the existence of ionic species. Although no hydrogen peroxide was detected in PAW and PAB, the microbial reductions observed with these solutions, suggested the presence of other potent antimicrobial species.

Surface roughness clearly played a role in microbial inactivation efficacy of PAB, however the results obtained with PAW, were less conclusive and can in part be attributed to the high variability observed in microbial inactivation on different surfaces. Further research on PAW and PAB, is needed to determine their suitability as industrial sanitizers.

5. FUTURE WORK

To determine the suitability of PAW and PAB, it would be important to characterize the plasma chemistry for buffer systems. Effect of other factors that may affect sanitizer efficacy, including organic load and bacterial strain or species need to be studied further. Techniques to better identify the surface wetting properties of fresh produce may help us better understand the interaction of plasma species and produce surface properties on microbial inactivation. Moreover, the use of plasma to activate buffers made with different organic acids may prove interesting, as the inherent antimicrobial capacity of organic acids, may be enhanced with plasma treatment.

6. REFERENCES

1. Anderson, C. E., Cha, N. R., Lindsay, A. D., Clark, D. S., & Graves, D. B. (2016). The Role of Interfacial Reactions in Determining Plasma–Liquid Chemistry. *Plasma Chemistry and Plasma Processing*, 36(6), 1393-1415.
2. B.C. MacDonald & Company, 2010. Available at: http://www.dphu.org/uploads/attachements/books/books_2958_0.pdf. Accessed on 01/21/2017.
3. Bai, N., Sun, P., Zhou, H., Wu, H., Wang, R., Liu, F., Zhu, W., Lopez, J., Zhang, J., & Fang, J. (2011). Inactivation of Staphylococcus aureus in water by a cold, He/O2 atmospheric pressure plasma microjet *Plasma Processes and Polymers*, 8(5), 424-431.
4. Beckert, S. F. and Reitz, F. J. (2012). MSA method application in evaluating of measurement system used to measure the roughness parameter *Ra*. *15th International Conference on Experimental Mechanics*. Paper Ref: 3092.
5. Beuchat, L. (1998). Surface decontamination of fruits and vegetables eaten raw: a review. In *Surface decontamination of fruits and vegetables eaten raw: a review*. OMS.
6. Bhide, S. (2016). *Effect of surface roughness in model and fresh fruit systems on microbial inactivation efficacy of cold atmospheric pressure plasma* (Doctoral dissertation, Rutgers University-Graduate School-New Brunswick).
7. Burlica, R., Grim, R. G., Shih, K. Y., Balkwill, D., & Locke, B. R. (2010). Bacteria inactivation using low power pulsed gliding arc discharges with water spray. *Plasma Processes and Polymers*, 7(8), 640-649.
8. Center for Disease Control and Prevention (2013). Overview of Foodborne Disease Outbreaks, 2013. Available at https://www.cdc.gov/foodsafety/fdoss/data/annual-summaries/mmwr-questions-and-answers-2013.html. Accessed on 12/3/2016
9. Center for Disease Control and Prevention (2016). Reports of Selected Salmonella Outbreak Investigations. Available at http://www.cdc.gov/salmonella/outbreaks.html. Accessed on 12/3/2016
10. Centers for Disease Control and Prevention, (2017). List of Selected Multistate Foodborne Outbreak Investigations. Available at: https://www.cdc.gov/foodsafety/outbreaks/multistate-outbreaks/outbreaks-list.html. Accessed on: 01/25/2017.
11. Chau, T. T., Kao, K. C., Blank, G., & Madrid, F. (1996). Microwave plasmas for low-temperature dry sterilization. *Biomaterials*, 17(13), 1273-1277.
12. Chemicool (2017). *Definition of Atomic-emission spectroscopy* (AES, OES). Available at: http://www.chemicool.com/definition/atomic_emission_spectroscopy_aes_oes.html. Accessed on 01/21/2017
13. Chen, Y., Jackson, K. M., Chea, F. P., & Schaffner, D. W. (2001). Quantification and variability analysis of bacterial cross-contamination rates in common food service tasks. *Journal of Food Protection®*, *64*(1), 72-80.

14. Claxton, N. S., Fellers, T. J., & Davidson, M. W. (2006). Laser scanning confocal microscopy. *Department of Optical Microscopy and Digital Imaging, Florida State University, Tallahassee,* Available at: *http://www. olympusconfocal. com/theory/LSCMIntro. pdf.*
15. d'Agostino, R., Favia, P., Oehr, C., & Wertheimer, M. R. (2005). Low-Temperature Plasma Processing of Materials: Past, Present, and Future. *Plasma Processes and Polymers*, 2(1), 7-15.
16. Danyluk, M. D., & Schaffner, D. W. (2011). Quantitative assessment of the microbial risk of leafy greens from farm to consumption: preliminary framework, data, and risk estimates. *Journal of food protection*, *74*(5), 700-708.
17. Dhawan, V. (2014). Reactive Oxygen and Nitrogen Species: General Considerations. In *Studies on Respiratory Disorders* (pp. 27-47). Springer New York.
18. Dove, J. E., Frost, J. D., & Dove, P. M. (1996). Geomembrane microtopography by atomic force microscopy. *Geosynthetics International*, 3(2), 227-245.
19. Dürrenberger, M. B., Handschin, S., Conde-Petit, B., & Escher, F. (2001). Visualization of food structure by confocal laser scanning microscopy (CLSM). *LWT-Food Science and Technology*, 34(1), 11-17.
20. Eisenberg, G. (1943). Colorimetric determination of hydrogen peroxide. *Industrial & Engineering Chemistry Analytical Edition*, 15(5), 327-328.
21. Emerson Process Management, (2008). Fundamentals of ORP measurement. Available at: http://www2.emersonprocess.com/siteadmincenter/PM%20Rosemount%20Analytical%20Documents/Liq_ADS_43-014.pdf. Accessed on 01/22/2017.
22. Emerson Process Management, (2010). Theory and application of conductivity. Available at: http://www.emerson.com/resource/blob/68442/7b95542772c37c1415ce2ff0a3c4521a/application-data--theory-and-application-of-conductivity-data.pdf. Accessed on 01/22/2017.
23. FAO, (1986). *Improvement of Post-Harvest Fresh Fruits and Vegetables Handling*. Regional Office for Asia and the Pacific. Maliwan Mansion, Phra Atit Road, Bangkok, 10200, Thailand.
24. Gaunt, L. F., Beggs, C. B., & Georghiou, G. E. (2006). Bactericidal action of the reactive species produced by gas-discharge nonthermal plasma at atmospheric pressure: a review. *IEEE Transactions on Plasma Science*, 34(4), 1257-1269.
25. Gil, M. I., Allende, A., & Selma, M. V. (2011). Treatments to ensure safety of fresh-cut fruits and vegetables. *Advances in fresh-cut fruits and vegetables processing*, 211-229.
26. Graves Lab, 2013. Peroxide (H_2O_2) Quantification. Available at: http://www.graveslab.org/lab-resources/procedures/peroxide-h2o2-quantification; Accessed on 12/05/2016
27. Haber, F., & Weiss, J. (1934). The catalytic decomposition of hydrogen peroxide by iron salts. In *Proceedings of the Royal Society of London A: Mathematical, Physical and Engineering Sciences* (Vol. 147, No. 861, pp. 332-351). The Royal Society.

28. Halprin, K. M., & Ohkawara, A. (1967). The Measurement of Glutathione in Human Epidermis Using Glutathione Reductase1. *Journal of Investigative Dermatology*, 48(2), 149-152.
29. Herdt, J., & Feng, H. (2009). Aqueous antimicrobial treatments to improve fresh and fresh-cut produce safety. *Microbial safety of fresh produce*. Wiley-Blackwell, Ames, IA, 169-190.
30. Houpt, P. M., & Draaijer, A. (1989). *U.S. Patent No. 4,863,226*. Washington, DC: U.S. Patent and Trademark Office.
31. International Organization of Standardization (ISO) (Organisation internationale de normalization). (1997). *Geometrical Product Specifications (GPS)--Surface Texture: Profile Method--Terms, Definitions and* Surface Texture Parameters. International Organization for Standardization.
32. Joshi, S. G., Cooper, M., Yost, A., Paff, M., Ercan, U. K., Fridman, G., Friedman, G., Fridman, A. & Brooks, A. D. (2011). Nonthermal dielectric-barrier discharge plasma-induced inactivation involves oxidative DNA damage and membrane lipid peroxidation in Escherichia coli. *Antimicrobial agents and chemotherapy*, 55(3), 1053-1062.
33. Kalghatgi, S., Tsai, C., Gray, R., & Pappas, D. (2015). Transdermal drug delivery using cold plasmas. In *22nd International Symposium on Plasma Chemistry* (pp. 5-10).
34. Kamgang-Youbi, G., Herry, J. M., Bellon-Fontaine, M. N., Brisset, J. L., Doubla, A., & Naïtali, M. (2007). Evidence of temporal postdischarge decontamination of bacteria by gliding electric discharges: application to *Hafnia alvei. Applied and environmental microbiology*, 73(15), 4791-4796.
35. Kamgang-Youbi, G., Herry, J. M., Brisset, J. L., Bellon-Fontaine, M. N., Doubla, A., & Naïtali, M. (2008). Impact on disinfection efficiency of cell load and of planktonic/adherent/detached state: case of *Hafnia alvei* inactivation by Plasma Activated Water. *Applied microbiology and biotechnology*, 81(3), 449-457.
36. Kamgang-Youbi, G., Herry, J. M., Meylheuc, T., Brisset, J. L., Bellon-Fontaine, M. N., Doubla, A., & Naitali, M. (2009). Microbial inactivation using plasma-activated water obtained by gliding electric discharges. *Letters in applied microbiology*, 48(1), 13-18.
37. Kirkpatrick, M. J., & Locke, B. R. (2005). Hydrogen, oxygen, and hydrogen peroxide formation in aqueous phase pulsed corona electrical discharge. *Industrial & engineering chemistry research*, 44(12), 4243-4248.
38. Kitinoja, L., & Kader, A. A. (2002). *Small-scale postharvest handling practices: a manual for horticultural crops*. University of California, Davis, Postharvest Technology Research and Information Center.
39. Kramida, A., Ralchenko, Yu., Reader, J. and NIST ASD Team (20l6). *NIST Atomic Spectra Database* (version 5.4), [Online]. Available: http://physics.nist.gov/asd [Mon Dec 05 2016]. National Institute of Standards and Technology, Gaithersburg, MD
40. Lang, M. M., Harris, L. J., & Beuchat, L. R. (2004). Evaluation of inoculation method and inoculum drying time for their effects on survival and efficiency of recovery of Escherichia coli O157: H7, Salmonella, and Listeria monocytogenes inoculated on the surface of tomatoes. *Journal of Food Protection®*, 67(4), 732-741.

41. Langmuir, I. (1928). Oscillations in ionized gases. *Proceedings of the National Academy of Sciences*, 14(8), 627-637.
42. Laroussi, M., & Leipold, F. (2004). Evaluation of the roles of reactive species, heat, and UV radiation in the inactivation of bacterial cells by air plasmas at atmospheric pressure. *International Journal of Mass Spectrometry*, 233(1), 81-86.
43. Liao, L. B., Chen, W. M., & Xiao, X. M. (2007). The generation and inactivation mechanism of oxidation–reduction potential of electrolyzed oxidizing water. *Journal of Food Engineering*, 78(4), 1326-1332.
44. Linley, E., Denyer, S. P., McDonnell, G., Simons, C., & Maillard, J. Y. (2012). Use of hydrogen peroxide as a biocide: new consideration of its mechanisms of biocidal action. *Journal of antimicrobial chemotherapy*, 67(7), 1589-1596
45. Liu, B., & Schaffner, D. W. (2007). Quantitative analysis of the growth of Salmonella Stanley during alfalfa sprouting and evaluation of Enterobacter aerogenes as its surrogate. *Journal of Food Protection®*, *70*(2), 316-322.
46. Liu, D. X., Liu, Z. C., Chen, C., Yang, A. J., Li, D., Rong, M. Z., Chen, H. L., & Kong, M. G. (2016). Aqueous reactive species induced by a surface air discharge: Heterogeneous mass transfer and liquid chemistry pathways. *Scientific reports*, 6.
47. Loureiro, J., & Amorim, J. (2016). Applications of Low-Temperature Plasmas. In *Kinetics and Spectroscopy of Low Temperature Plasmas* (pp. 413-440). Springer International Publishing.
48. Lukes, P., Clupek, M., Babicky, V., & Sunka, P. (2008). Ultraviolet radiation from the pulsed corona discharge in water. *Plasma sources science and technology*, 17(2), 024012.
49. Ma, R., Wang, G., Tian, Y., Wang, K., Zhang, J., & Fang, J. (2015). Non-thermal plasma-activated water inactivation of food-borne pathogen on fresh produce. *Journal of hazardous materials*, 300, 643-651.
50. Ma, R., Wang, G., Tian, Y., Wang, K., Zhang, J., & Fang, J. (2015). Non-thermal plasma-activated water inactivation of food-borne pathogen on fresh produce. *Journal of hazardous materials*, 300, 643-651.
51. Machala, Z., Tarabova, B., Hensel, K., Spetlikova, E., Sikurova, L., & Lukes, P. (2013). Formation of ROS and RNS in Water Electro-Sprayed through Transient Spark Discharge in Air and their Bactericidal Effects. *Plasma Processes and Polymers*, 10(7), 649-659.
52. MacNevin, D. E. (2007). *The effects of phosphate and silicate inhibitors on surface roughness and copper release in water distribution systems*. ProQuest.
53. Maksimov, A. I., & Nikiforov, A. Y. (2007). Comparison of plasma and plasma-solution modifications of polymer materials in the liquid phase. *High Energy Chemistry*, 41(6), 454-459.
54. McPherson, L. L. (1993). Understanding ORP's role in the disinfection process. *Water engineering & management*, 140(11), 29-31.
55. Mertens, K., & Samuel, J. E. (2012). Defense mechanisms against oxidative stress in Coxiella burnetii: adaptation to a unique intracellular niche. In *Coxiella burnetii: Recent Advances and New Perspectives in Research of the Q Fever Bacterium* (pp. 39-63). Springer Netherlands.

56. Misra, N. N., Tiwari, B. K., Raghavarao, K. S. M. S., & Cullen, P. J. (2011). Nonthermal plasma inactivation of food-borne pathogens. *Food Engineering Reviews*, 3(3-4), 159-170.
57. Montenegro, J., Ruan, R., Ma, H., & Chen, P. (2002). Inactivation of E. coli O157: H7 using a pulsed nonthermal plasma system. *Journal of food science*, 67(2), 646-648.
58. Moreau, M., Orange, N., & Feuilloley, M. G. J. (2008). Non-thermal plasma technologies: new tools for bio-decontamination. *Biotechnology advances*, 26(6), 610-617.
59. Naïtali, M., Kamgang-Youbi, G., Herry, J. M., Bellon-Fontaine, M. N., & Brisset, J. L. (2010). Combined effects of long-living chemical species during microbial inactivation using atmospheric plasma-treated water. *Applied and environmental microbiology*, 76(22), 7662-7664.
60. Oehmigen, K., Hähnel, M., Brandenburg, R., Wilke, C., Weltmann, K. D., & Von Woedtke, T. (2010). The role of acidification for antimicrobial activity of atmospheric pressure plasma in liquids. *Plasma Processes and Polymers*, 7(3-4), 250-257.
61. Oliver, R., Jones, R., Gray, D., (1994). Oxidation Reduction Potential. In Liptak, B., *Analytical Instrumentation*. pp 268-273. CRC Press.
62. Painter, J., Hoekstra, R., Ayers, T., Tauxe, R., Braden, C., Angulo, F., and Griffin, P. (2013). Attribution of Foodborne Illnesses, Hospitalizations, and Deaths to Food Commodities by using Outbreak Data, United States, 1998–2008. *Emerging Infectious Diseases*, 19(3), 407-415.
63. Pankaj, S. K., Bueno-Ferrer, C., Misra, N. N., Milosavljević, V., O'Donnell, C. P., Bourke, P., Keener K.M., & Cullen, P. J. (2014). Applications of cold plasma technology in food packaging. *Trends in Food Science & Technology*, 35(1), 5-17.
64. Plasmatreat USA Inc., 2016. Plasma system and components. Available at http://www.plasmatreat.com/plasma-system-components/plasma-nozzles_for_cold-plasma-generation.html. Accessed on 12/04/2016
65. Radiometer Analytical SAS, (2004). Conductivity - Theory and Practice. Available at: http://www.analytical-chemistry.uoc.gr/files/items/6/618/agwgimometria_2.pdf. Accessed on 01/22/2017.
66. Ragni, L., Berardinelli, A., Vannini, L., Montanari, C., Sirri, F., Guerzoni, M. E., & Guarnieri, A. (2010). Non-thermal atmospheric gas plasma device for surface decontamination of shell eggs. *Journal of Food Engineering*, 100(1), 125-132.
67. Satterfield, C. N., & Bonnell, A. H. (1955). Interferences in titanium sulfate method for hydrogen peroxide. *Analytical Chemistry*, 27(7), 1174-1175.
68. Schafer, F. Q., & Buettner, G. R. (2001). Redox environment of the cell as viewed through the redox state of the glutathione disulfide/glutathione couple. *Free Radical Biology and Medicine*, 30(11), 1191-1212.
69. Schnabel, U., Andrasch, M., Weltmann, K. D., & Ehlbeck, J. (2014). Inactivation of vegetative microorganisms and Bacillus atrophaeus endospores by reactive nitrogen species (RNS). *Plasma Processes and Polymers*, 11(2), 110-116.

70. Scholtz, V., Pazlarova, J., Souskova, H., Khun, J., & Julak, J. (2015). Nonthermal plasma—a tool for decontamination and disinfection. *Biotechnology advances*, 33(6), 1108-1119.
71. Shen, J., Tian, Y., Li, Y., Ma, R., Zhang, Q., Zhang, J., & Fang, J. (2016). Bactericidal Effects against S. aureus and Physicochemical Properties of Plasma Activated Water stored at different temperatures. *Scientific Reports*, 6.
72. Shi, X. M., Zhang, G. J., Wu, X. L., Li, Y. X., Ma, Y., & Shao, X. J. (2011). Effect of low-temperature plasma on microorganism inactivation and quality of freshly squeezed orange juice. *IEEE Transactions on Plasma Science*, 39(7), 1591-1597.
73. Stoffels, E., Gonzalvo, Y. A., Whitmore, T. D., Seymour, D. L., & Rees, J. A. (2007). Mass spectrometric detection of short-living radicals produced by a plasma needle. *Plasma Sources Science and Technology*, 16(3), 549.
74. Suchentrunk, R., Staudigl, G., Jonke, D., & Fuesser, H. J. (1997). Industrial applications for plasma processes—examples and trends. *Surface and Coatings Technology*, 97(1), 1-9.
75. Surowsky, B., Fröhling, A., Gottschalk, N., Schlüter, O., & Knorr, D. (2014). Impact of cold plasma on Citrobacter freundii in apple juice: Inactivation kinetics and mechanisms. *International journal of food microbiology*, 174, 63-71.
76. Surowsky, B., Schlüter, O., & Knorr, D. (2015). Interactions of non-thermal atmospheric pressure plasma with solid and liquid food systems: a review. *Food Engineering Reviews*, 7(2), 82-108.
77. Tatarova, E., Dias, F. M., Felizardo, E., Henriques, J., Pinheiro, M. J., Ferreira, C. M., & Gordiets, B. (2010). Microwave air plasma source at atmospheric pressure: Experiment and theory. *Journal of Applied Physics*, 108(12), 123305.
78. Tian, Y., Ma, R., Zhang, Q., Feng, H., Liang, Y., Zhang, J., & Fang, J. (2015). Assessment of the Physicochemical Properties and Biological Effects of Water Activated by Non-thermal Plasma Above and Beneath the Water Surface. *Plasma Processes and Polymers,* 12(5), 439-449.
79. Traylor, M. J., Pavlovich, M. J., Karim, S., Hait, P., Sakiyama, Y., Clark, D. S., & Graves, D. B. (2011). Long-term antibacterial efficacy of air plasma-activated water. *Journal of Physics D: Applied Physics, 44*(47), 472001.
80. U.S. Food and Drug Administration (FDA), (2008). Guidance for Industry: Guide to Minimize Microbial Food Safety Hazards of Fresh-cut Fruits and Vegetables. Available at: http://www.fda.gov/Food/GuidanceRegulation/GuidanceDocumentsRegulatoryInformation/ProducePlantProducts/ucm064458.htm. Accessed on 01/25/2017.
81. U.S. Food and Drug Administration (FDA), (2014). Chapter V. Methods to Reduce/Eliminate Pathogens from Produce and Fresh-Cut Produce. Available at: https://www.fda.gov/Food/FoodScienceResearch/SafePracticesforFoodProcesses/ucm091363.htm. Accessed on: 03/01/2017
82. U.S. Food and Drug Administration (FDA), (2015a). Analysis and Evaluation of Preventive Control Measures for the Control and Reduction/Elimination of Microbial Hazards on Fresh and Fresh-Cut Produce: Chapter IV. Outbreaks Associated with Fresh and Fresh-Cut Produce. Incidence, Growth, and Survival of Pathogens in Fresh

and Fresh-Cut Produce. Available at: http://www.fda.gov/Food/FoodScienceResearch/SafePracticesforFoodProcesses/ucm091265.htm. Accessed on 02/05/2017.

83. U.S. Food and Drug Administration (FDA), (2015b). Inventory of Effective Food Contact Substance (FCS) Notifications. *FCN No. 1470*. Available at: https://www.accessdata.fda.gov/scripts/fdcc/?set=FCN&id=1470. Accessed on: 02/16/2017.
84. United States Department of Agriculture (2016). *An integrated approach to eliminate cross-contamination during washing, conveying, handling and packaging of fresh produce*. Available on: http://portal.nifa.usda.gov/web/crisprojectpages/1005370-an-integrated-approach-to-eliminate-cross-contamination-during-washing-conveying-handling-and-packaging-of-fresh-produce.html. Accessed on: 01/27/2017
85. United States Department of Agriculture (2017). Food Safety and Inspection Service. Safe and suitable ingredients used in the production of meat, poultry, and egg products. *FSIS Directive 7120.1 Rev.37.* Available on: https://www.fsis.usda.gov/wps/wcm/connect/bab10e09-aefa-483b-8be8-809a1f051d4c/7120.1.pdf?MOD=AJPERES. Accessed on: 02/16/2017.
86. Van Gils, C. A. J., Hofmann, S., Boekema, B. K. H. L., Brandenburg, R., & Bruggeman, P. J. (2013). Mechanisms of bacterial inactivation in the liquid phase induced by a remote RF cold atmospheric pressure plasma jet. *Journal of Physics D: Applied Physics*, 46(17), 175203.
87. von Woedtke, T., Haertel, B., Weltmann, K. D., & Lindequist, U. (2013). Plasma pharmacy–physical plasma in pharmaceutical applications. *Die Pharmazie-An International Journal of Pharmaceutical Sciences*, 68(7), 492-498.
88. Wang, H., Feng, H., Liang, W., Luo, Y., & Malyarchuk, V. (2009). Effect of surface roughness on retention and removal of Escherichia coli O157: H7 on surfaces of selected fruits*. Journal of food science*, 74(1).
89. Xu, Y., Tian, Y., Ma, R., Liu, Q., & Zhang, J. (2016). Effect of plasma activated water on the postharvest quality of button mushrooms, Agaricus bisporus. *Food chemistry*, 197, 436-444.
90. Xu, Y., Tian, Y., Ma, R., Liu, Q., & Zhang, J. (2016). Effect of plasma activated water on the postharvest quality of button mushrooms, *Agaricus bisporus. Food chemistry*, 197, 436-444.
91. Zhang, Q., Liang, Y., Feng, H., Ma, R., Tian, Y., Zhang, J., & Fang, J. (2013). A study of oxidative stress induced by non-thermal plasma-activated water for bacterial damage. *Applied Physics Letters*, 102(20), 203701.
92. Zhao, P., Zhao, T., Doyle, M. P., Rubino, J. R., & Meng, J. (1998). Development of a model for evaluation of microbial cross-contamination in the kitchen. *Journal of Food Protection®*, *61*(8), 960-963.